

---

NOAA Technical Memorandum NWS WR-284

**THE PRESIDENTS' DAY 2005 TORNADOES IN THE SOUTHERN  
SACRAMENTO VALLEY OF NORTHERN CALIFORNIA**

James H. Mathews  
September 2009

Weather Forecast Office Sacramento, CA

*United States  
Department of Commerce  
Gary Locke, Secretary*

*National Oceanic and  
Atmospheric Administration  
Dr. Jane Lubchenco  
Under Secretary*

*National Weather Services  
Dr. John (Jack) Hayes, Assistant Administrator  
for Weather Services*

And is approved for publication by  
Scientific Services Division  
Western Region

Andy Edman, Chief  
Scientific Services Division  
Salt Lake City, UT

# THE PRESIDENTS' DAY 2005 TORNADOES IN THE SOUTHERN SACRAMENTO VALLEY OF NORTHERN CALIFORNIA

James H. Mathews  
National Weather Service  
Weather Forecast Office Sacramento, CA

## 1. INTRODUCTION

On 21 February 2005 Presidents' Day, three tornadoes and several funnel clouds occurred in the Sacramento valley, including two weak (F0\*) tornadoes in the Sacramento, CA metropolitan area. The Southport, CA and Natomas, CA tornadoes caused nearly one million dollars of damage to residential and commercial property. Amazingly, there were no fatalities or serious injuries despite the amount of flying debris, air-borne projectiles, toppled trees, and an over-turned semi-trailer truck. Photographic evidence, and an examination of radar data post facto, confirmed there was a third tornado near Dunnigan, CA, in the rural portion of Yolo County (Fig. 1).

Compared to the area east of the Rocky Mountains, tornado occurrence over the western United States is much less frequent. However, climatological studies reveal certain sub-regions throughout the west where there is a significant increase in tornado occurrence. Two of the regions are in California: the Los Angeles area, and the Central Valley of California comprising the Sacramento and San Joaquin Valleys. Comparative climatological studies show that most California tornadoes are relatively weak (F0 or F1 intensity) and have relatively short path lengths, with median values 0.62 miles (1.0 km) long and 43 yards (39.3 m) wide compared to 4 miles (6.4 km) long and 170 yards (155.4 m) for Iowa tornadoes. Also, the vast majority of California tornadoes occur during the cool season and primarily between 1 PM and 3 PM local time (Blier and Batten 1994).

Many of the tornadoes in the Central Valley of California are associated with synoptic patterns that create favorable buoyancy and shear profiles conducive for supercell storms. Initially, the pattern was described in Monteverdi et al. (1988) and later documented with other tornadic storms in the state by Monteverdi et al. (2001 and 2003). However, there are also many California Central Valley tornadoes that do not form with isolated supercells. Nonsupercell tornadoes in California have been documented along horizontally sheared fronts, intersections of bow echoes, or when isolated nonsupercell storms intercept pre-existing vertical vorticity from topographic or solenoidal circulations found along outflow or sea breeze boundaries. Monteverdi (et al. 2003) believes that these nonsupercell tornadoes probably account for a relatively large percentage of tornadoes across California.

\*In 2005, the National Weather Service (NWS) used the longstanding Fujita (F) Scale to rate tornado damage. In the spring of 2007, the NWS adopted the Enhanced-Fujita (EF) Scale. This change did not affect the findings of this study.

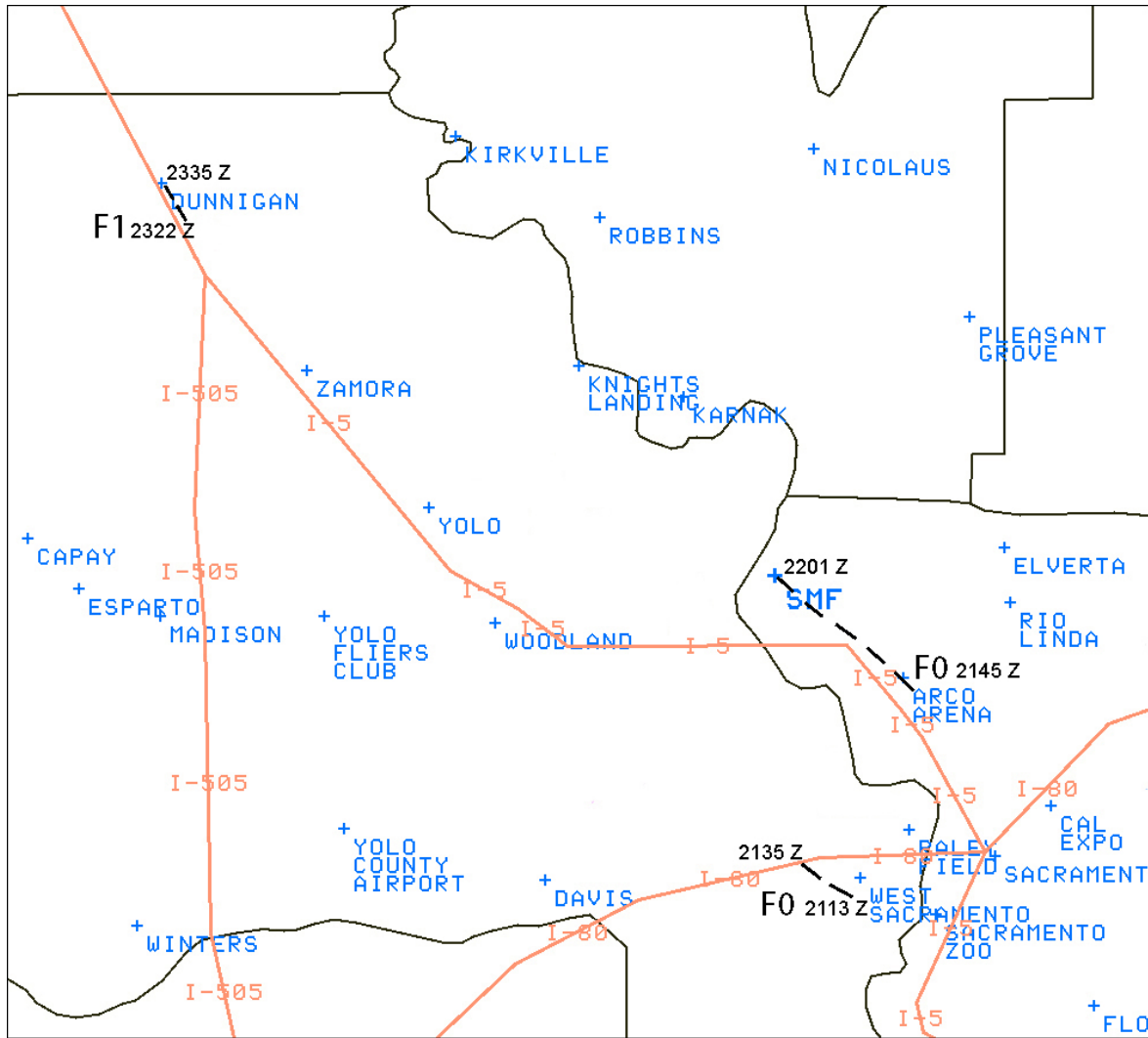


Figure 1

*Locations and times of tornadoes, intensities and paths. Tornado intensity (F0 or F1) shown with path and times of occurrence (Z or UTC). See text for details.*

This study will consider the meteorological factors that resulted in a rare weather event that was highly publicized by the local media. Low level shear and buoyancy parameters on 21 February 2005 were typical for northern California tornadoes (Monteverdi et al. 2003). However, this event was unique in that thunderstorms moved westward due to deep east to southeast flow to the north of a closed upper-level low pressure center off the California coast. Radar data from the Weather Surveillance Radar-1988 Doppler (WSR-88D) located in Davis, CA (KDAX) will be examined to illustrate the locations and intensities of the weather phenomena that occurred on that day.

This paper will discuss the synoptic situation that resulted in the development of low-topped supercells in the Sacramento valley on 21 February 2005 in section 2. An examination of radar imagery from the WSR-88D in Davis, CA (KDAX) for the Southport, CA, Natomas, CA and Dunnigan, CA tornadoes will be presented in section 3.

Included in section 3 is a discussion on supercell movement and the hodographs for the Natomas, CA and Dunnigan, CA tornadoes. Section 4 is a summary and offers recommendations for operational forecasters.

## 2. SYNOPTIC SITUATION

The majority of California tornadoes are associated with F0/F1 damage and occur during the winter and spring months when tropopause heights are low (Blier and Batten 1994), and when certain low-level positive wind shear and buoyancy parameters are present (Lipari and Monteverdi 2000, Monteverdi et al. 2003). Northern California tornadoes typically occur in a favorable meteorological environment as shown in Figure 2. The location of the middle and upper level trough causes west to southwest winds that are perpendicular to the coastal range mountains. This produces a lee-side trough in the Central Valley. East of the lee-side trough, topographic channeling of the winds creates surface southeasterly flow which contributes to a favorable shear profile and strongly anticyclonically-curved hodographs. Instability is augmented by mid-level cold air advection from the upper-level trough and low-level warm air advection from the southeasterly winds north of the synoptic cold front and/or differential heating (Monteverdi and Quadros 1994). The supercell thunderstorms that form in this environment have been called low-topped or miniature supercells and have also been observed in many mid-latitude locations (Wicker and Cantrell, 1996).

For the Presidents' Day 2005 northern California tornadic event, a closed off mid- and upper-level vorticity maximum was located off the California coast for several days. This weather pattern resulted in an unstable air mass over northern California. The Lifted Index from the 1200Z 21 February 2005 Oakland, CA (KOAK) sounding was minus 1.2. The flow around the closed off mid- and upper-level vorticity maximum advected a subtropical moisture plume and resulted in precipitable water (PW) values near eight-tenths of an inch or 171% of normal over the area (Fig. 3). Upward vertical motion across northern California was aided by a vorticity lobe rotating northeast around the offshore vorticity maximum and by mass divergence in the left exit region of the upper level jet.

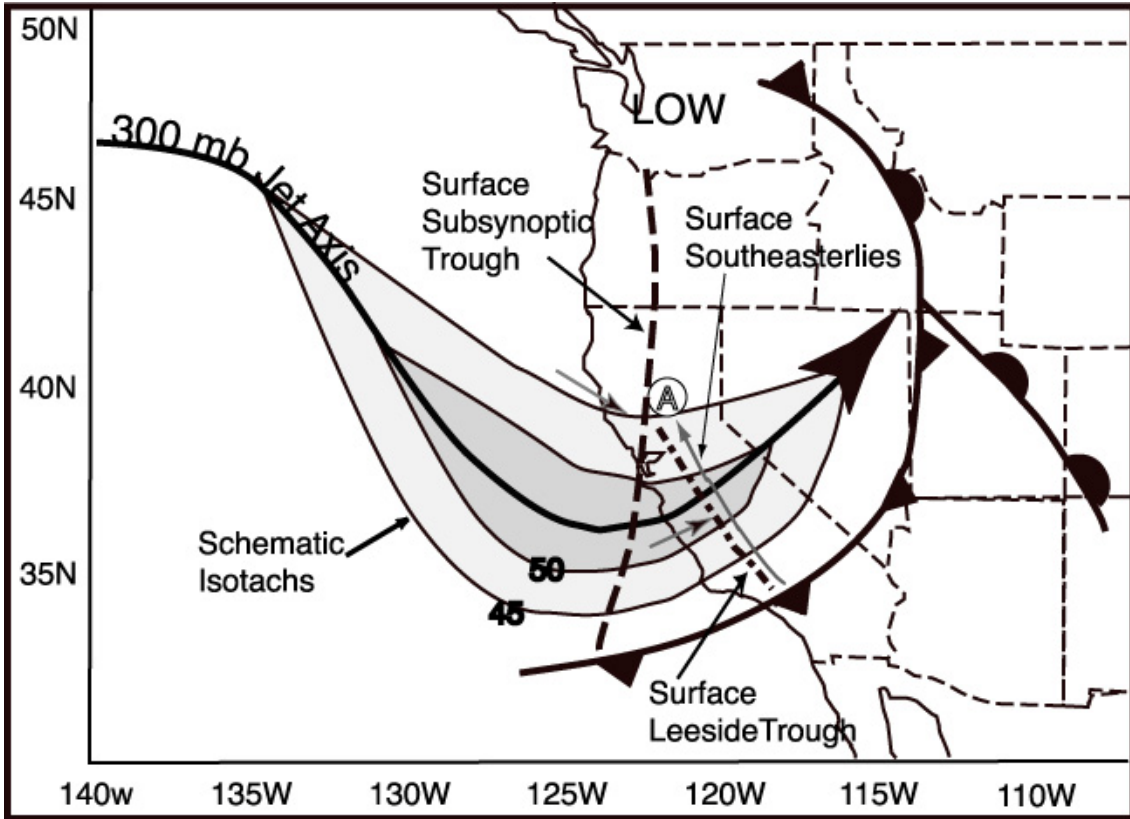


Figure 2

*Schematic showing the location of major synoptic features associated with tornadoes in the central valley of California (from Monteverdi et al. 2003).*

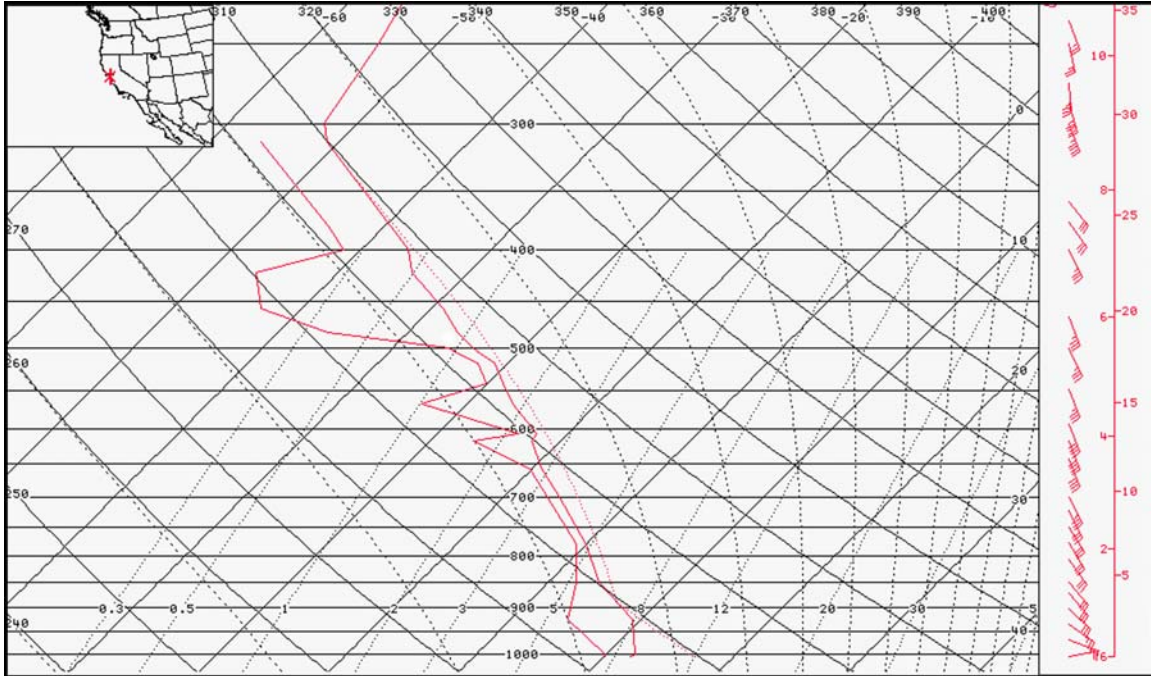


Figure 3  
 1200Z 21 February 2005 Oakland, CA (KOAK) Sounding. Wind barbs (far right) illustrate deep southeast flow (height in km and thousands of feet).

At the surface, an occluded front rotated northeast into the interior of northern California and provided a well defined boundary for the development of thunderstorms. A mid-level dry intrusion arced southeast to northwest into the southern Sacramento valley in the proximity of the occluded front. Differential heating caused a direct circulation in which warm air rises and cold air sinks, as cooler air from the cloud-covered areas north and east of the mid-level dry intrusion, flowed toward warmer air and lower pressure in the cloud-free areas immediately north and east of the occluded front (Fig. 4). The direct circulation resulted in an increased pressure gradient and produced a solenoidal circulation (Wolf 2002) believed to be an important factor in the generation of low-level shear and the initiation of severe convection in the Sacramento valley on 21 February 2005. In western Sacramento and Yolo counties, the solenoidal circulation caused light north winds at the surface, but southeast winds over eastern Sacramento County. This significantly increased the surface convergence and low-level wind shear over the western portion of Sacramento County from 2000Z to 2100Z, less than an hour prior to the Southport, CA and Natomas, CA tornadoes. The Local Area Processing Analyses (LAPS) surface streamline and wind analyses (Figs. 5a and 5b) illustrate the increasing surface convergence.

The 1200Z 21 February 2005 ETA model BUFKIT forecast wind profile for Sacramento International Airport (KSMF) at 2100Z illustrates the low-level veering of winds from north to southeast, within the boundary layer, and deep southeast flow aloft. The forecast of increasing southeast winds over 30 knots up to around 2 km increases the 0-2 km shear to 30 m/s (15 m/s/km) (Fig. 6). Deep southeast flow is atypical from the west-southwest flow in the lower to middle troposphere that is typically associated with tornadic storms in

the Central Valley of northern California. Instead of a strong veering southeast to west-northwest wind profile and eastward moving storms the deep southeast flow resulted in strong speed shear and westward moving storms.

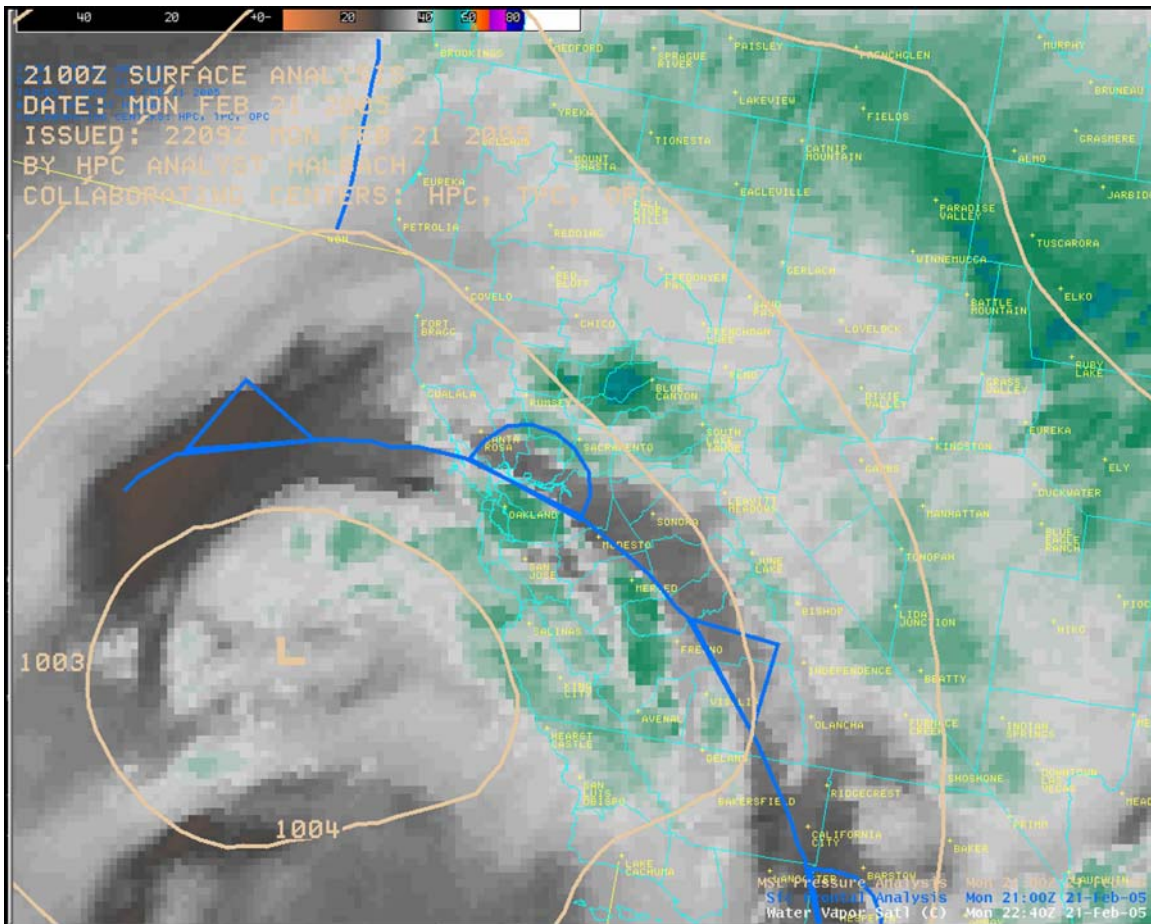


Figure 4  
 2240Z 21 February 2005 GOES West Water Vapor Satellite Imagery 2100Z MSL Pressure Analysis (tan) and Surface Frontal Analysis (blue).

The severe convection occurred on the “cool side” of the surface boundary where the Lifted Condensation Level (LCL) was low and moisture was pooling. Johns et al. (2000) found that low LCL heights and moisture pooling are common factors for tornadoes in the north central Great Plains. The 1200Z 21 February 2005 ETA model BUFKIT forecast sounding for Sacramento International Airport (KSMF) for 2100Z indicated a LCL of 980 hPa (around 300 meters), and the METAR data at 2100Z showed the highest dewpoint temperature, 56 degrees F (13.3 degrees C), at Sacramento International Airport (Fig. 7).

Markowski et al. (1998) found that the greatest tornado potential occurred from 10 km on the warm side of a boundary to 30 km on the cool side of the boundary, and the more shallow the boundary, the further into the cold air the tornado potential existed. Local

Area Processing Analyses (LAPS) streamline and wind analyses from 2000Z to 2100Z show a surface convergence zone moving from the eastern portion of Sacramento County into the northwest corner of the county, maximizing low level convergence near KSMF (Figs. 5a and 5b). Note the wind shift and rising pressure at Sacramento Executive Airport (KSAC) at 2200Z as the surface boundary moved from southeastern Sacramento County into the northwestern portion of the county. Also note the severe thunderstorm and tornado/funnel cloud present weather symbols on the KSMF weather observation (Fig. 8).

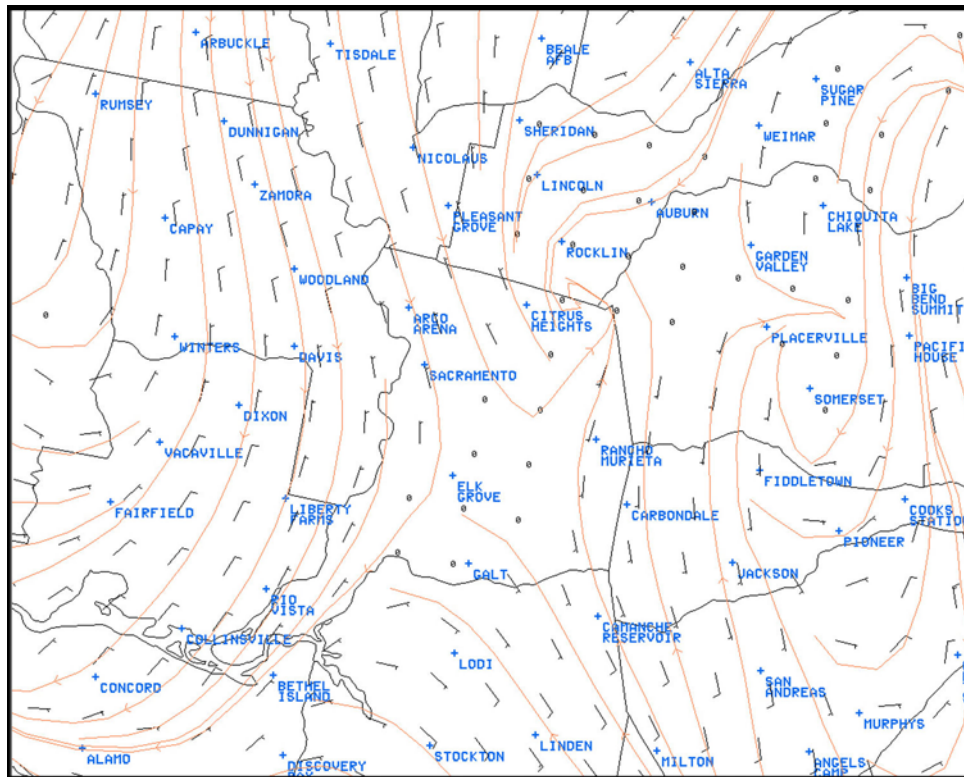


Figure 5a  
 2000Z 21 February 2005 LAPS Surface Wind (black) and Streamline Analysis (orange). Note meteorological col (saddle) over central Sacramento County indicating developing convergence boundary.

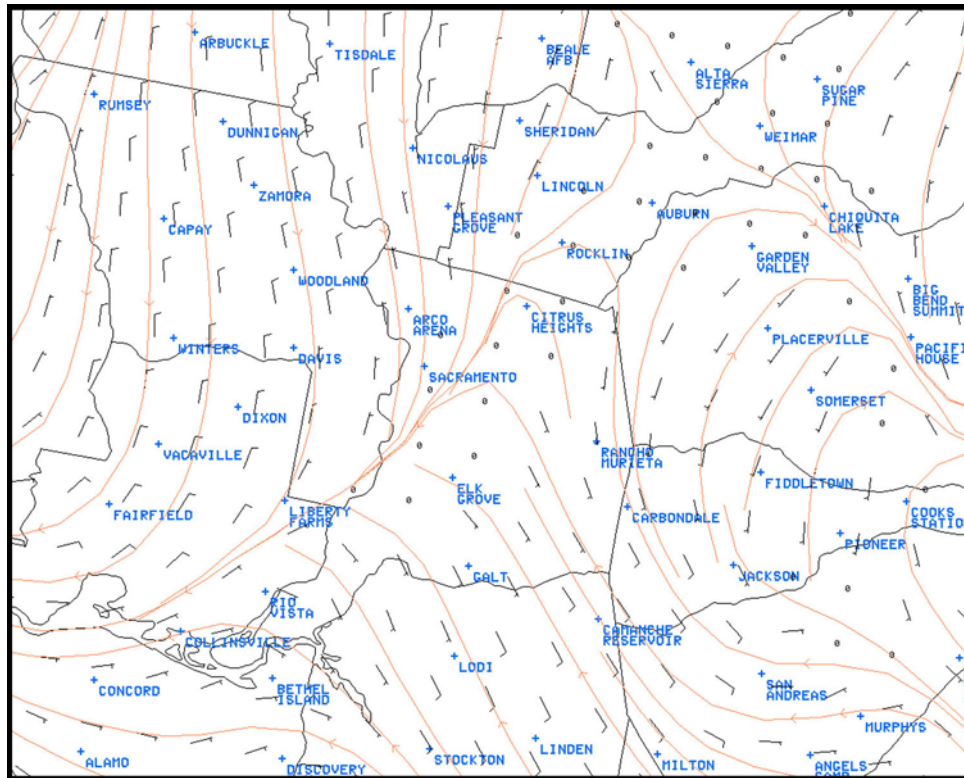


Figure 5b  
 2100Z 21 February 2005 LAPS Surface Wind (black) and Streamline  
 Analysis (orange). Note streamline convergence vicinity of Sacramento.

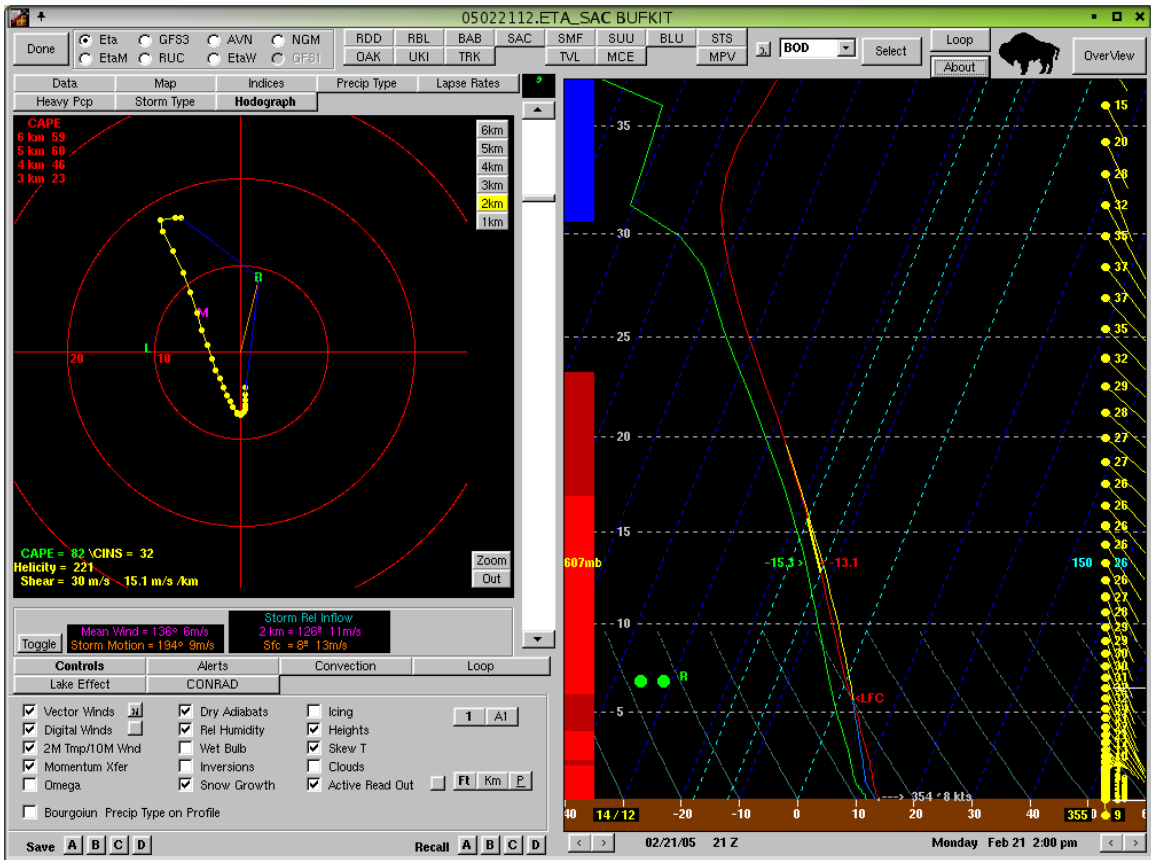


Figure 6  
 1200Z ETA BUFKIT Forecast for 2100Z 21 February 2005 for  
 Sacramento, CA (SAC).

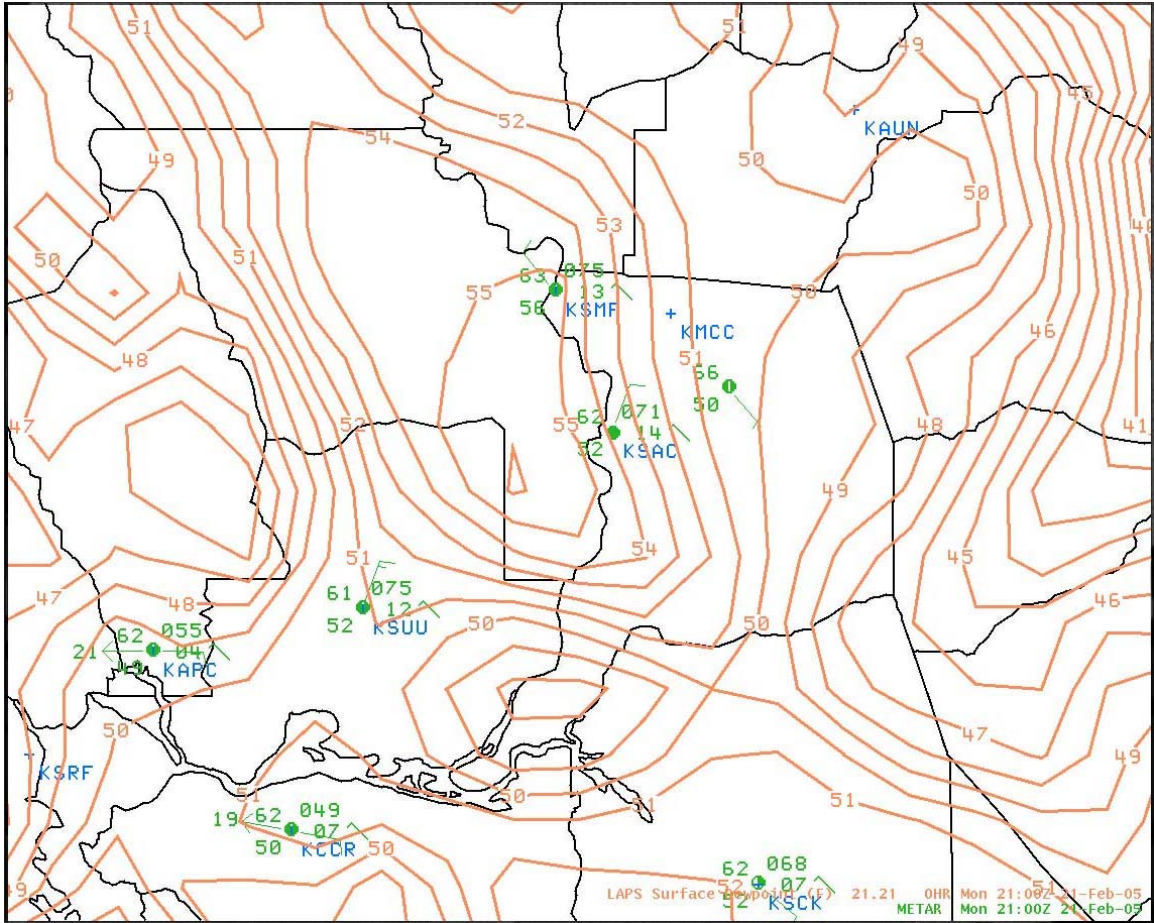


Figure 7  
 2100Z 21 February 2005 METAR Observations and LAPS Surface Dewpoint Isodrosotherms (tan lines). Note pooling of highest dewpoint temperatures west of Sacramento International Airport (KSMF) and Sacramento Executive Airport (KSAC).

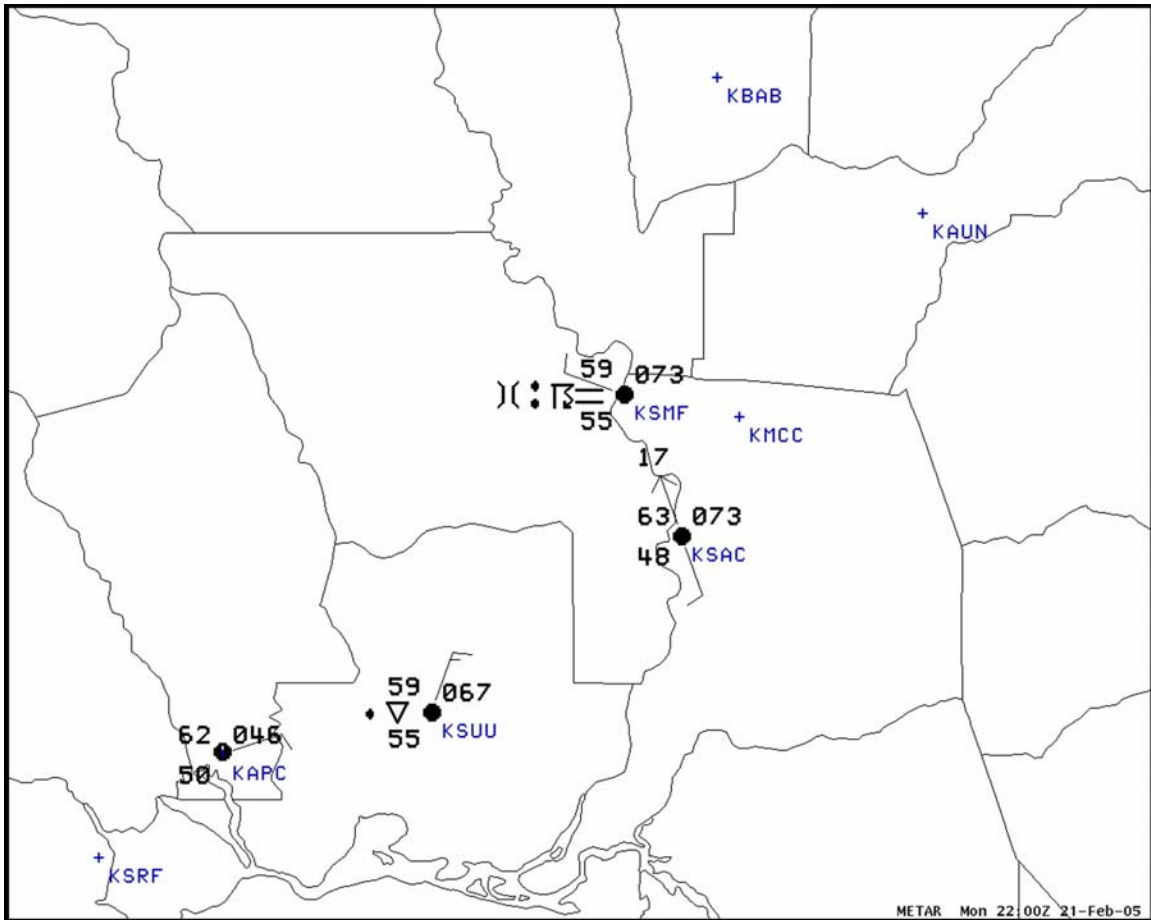


Figure 8  
 2200Z 21 February 2005 METAR Observations. Note Present Weather symbol  
 of Tornado/Funnel Cloud at Sacramento International Airport - KSMF.

Craven et al. (2002) found that tornado probability increases with increasing values of 0-1 km shear and decreasing LCL heights. Values from the 1200Z 21 February 2005 ETA model BUFKIT forecast sounding for 2100Z at KSMF showed 0-1 km shear of approximately 29 knots (around 15 meters/second), and a LCL height of 980 hPA (approximately 300 meters). Applying these data to the findings of Craven et al. (2002) in Table 1, the probability for a tornado was near 70%. Although the Craven et al. (2002) study was primarily intended for Great Plains supercells with moderate to strong instability, it has some applicability because of the instability and development of supercells in northern California on this date. Given favorable deep layer wind shear and adequate instability, forecasters can use this table to heighten their situational awareness for tornado potential.

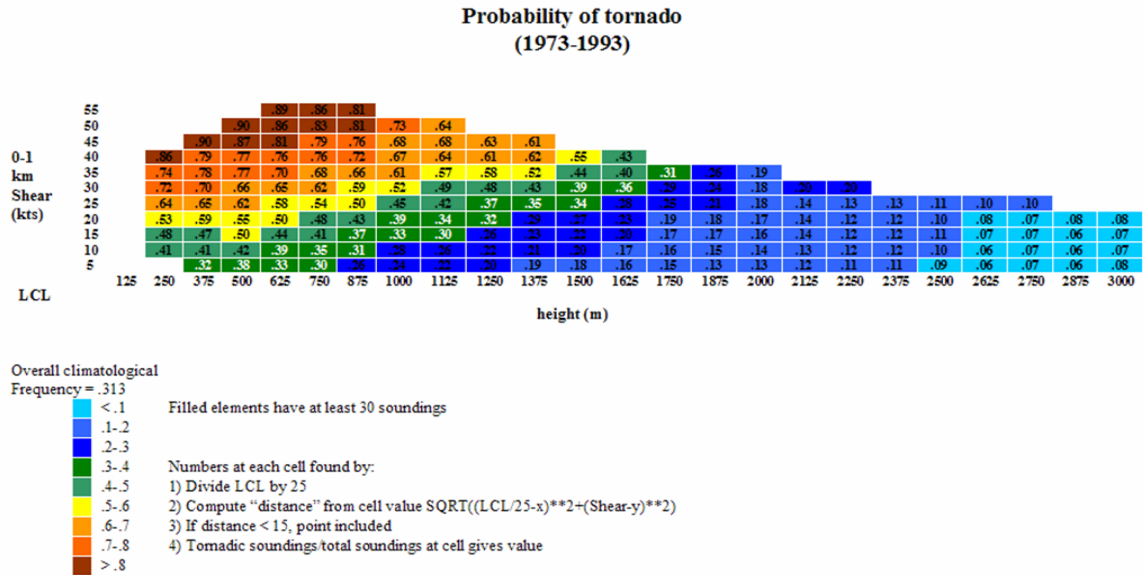


Figure 9  
*Craven et al. (2002) Probability of Tornado (study years 1973-1993)*  
*0-1 km Shear (knots) on x-axis and LCL (height in meters) on y-axis.*

Notice the 1200Z 21 February 2005 ETA model BUFKIT forecast hodograph for KSMF at 2100Z indicated a storm motion to the north (from 194 degrees) and a 0-2 km helicity value around 220 meters <sup>2</sup>/sec<sup>2</sup> (Fig. 6). The observed storm and forecast motions were to the west-northwest as a result of deep southeast flow. The positive shear values would favor an environment conducive to cyclonically rotating updrafts.

Surface winds from the northeast veering to the southeast and increasing significantly with height resulted in an anticyclonically-looping hodograph. In their research of northern and central California tornadoes during the period of 1990-1994, Lipari and Monteverdi (2000) found that the hodographs for tornadic storms in northern and central California often showed marked anticyclonic loops with strong veering of wind shear vectors with height. However, compare the 1200Z 21 February 2005 Oakland, CA (KOAK) sounding hodograph (Fig. 10) with the composite hodographs for F1/F2 tornadoes (Fig. 11) observed in other parts of the country (Davies 1993). Note the "loop" for 21 February 2005 is mostly contained in the in the upper-left quadrant of the hodograph, and is similar to the 1200Z 21 February 2005 ETA model BUFKIT forecast hodograph for KSMF at 2100Z (Fig. 6). The differences between the composite hodograph in Davies (1993) and the hodographs from 21 February 2005 are the result of light north-northeasterly surface winds seen in the METAR observations prior to the tornadoes, and the strong southeast flow aloft.

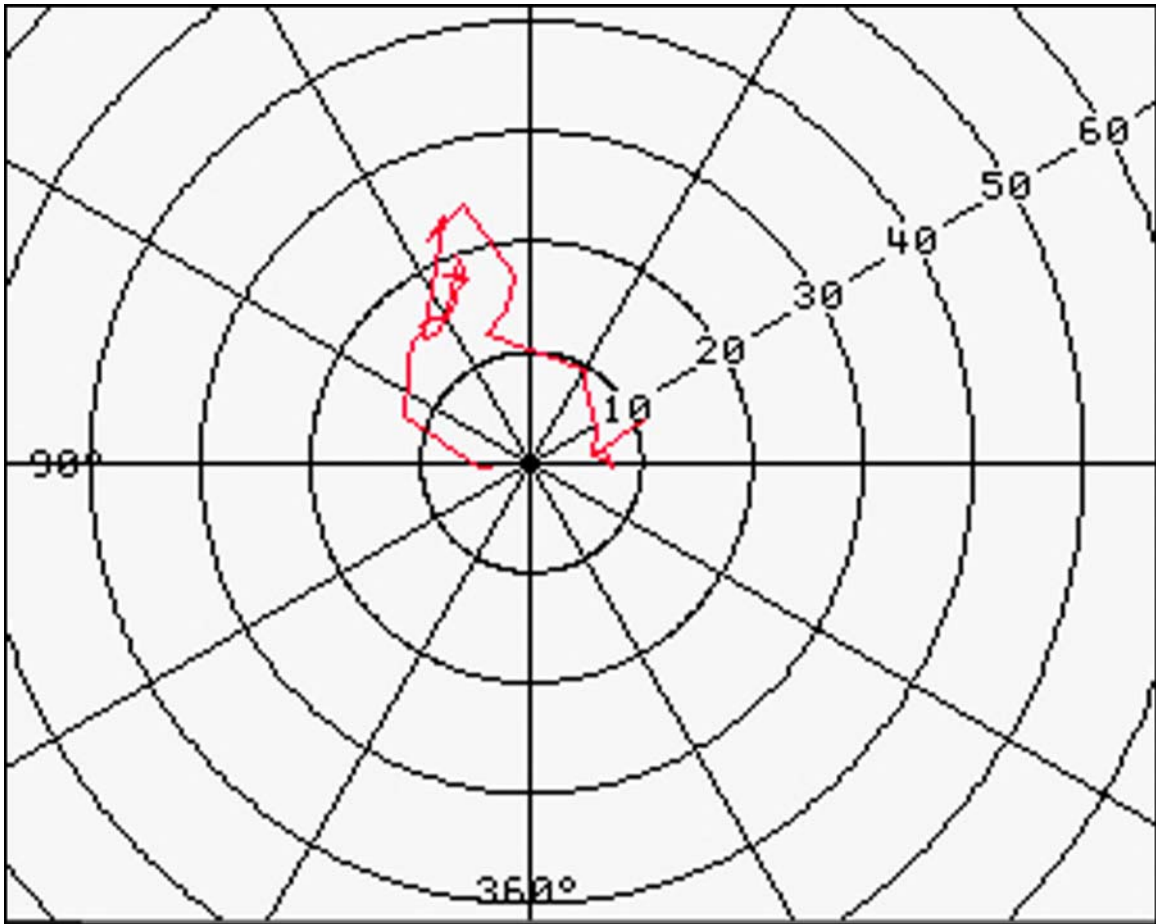


Figure 10  
*1200Z 21 February 2005 Oakland, CA (KOAK) Hodograph  
showing anticyclonically-curving loop.*

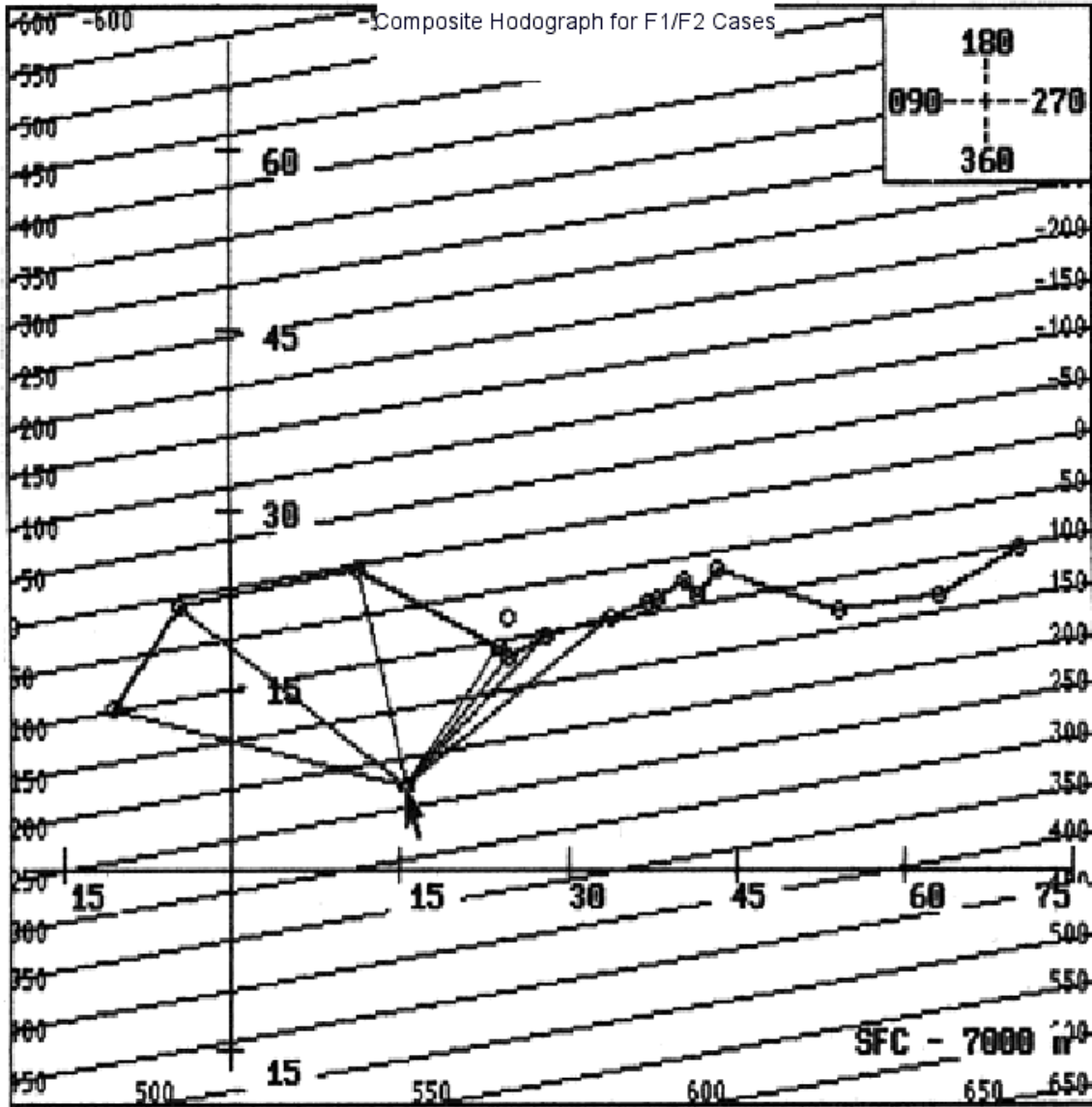


Figure 11  
*Composite Hodograph for F1/F2 Tornado Cases (Davies, 1993).*

Local Area Processing Analyses (LAPS) from 2000Z on 21 February 2005 quantitatively illustrated the location of the axis of instability and moisture convergence in the southern Sacramento valley (Figs. 12a- 12d). These figures indicate the tornadic activity that day occurred in a very unstable air mass and along the gradient of Convective Available Potential Energy (CAPE), surface moisture advection and moisture flux divergence, and not necessarily in the center of the highest value. Research by Broyles et al. (2002) Johns et al. (2000) and Thompson and Edwards (2000) discussed environmental conditions and locations of tornadoes and have noted similar findings.

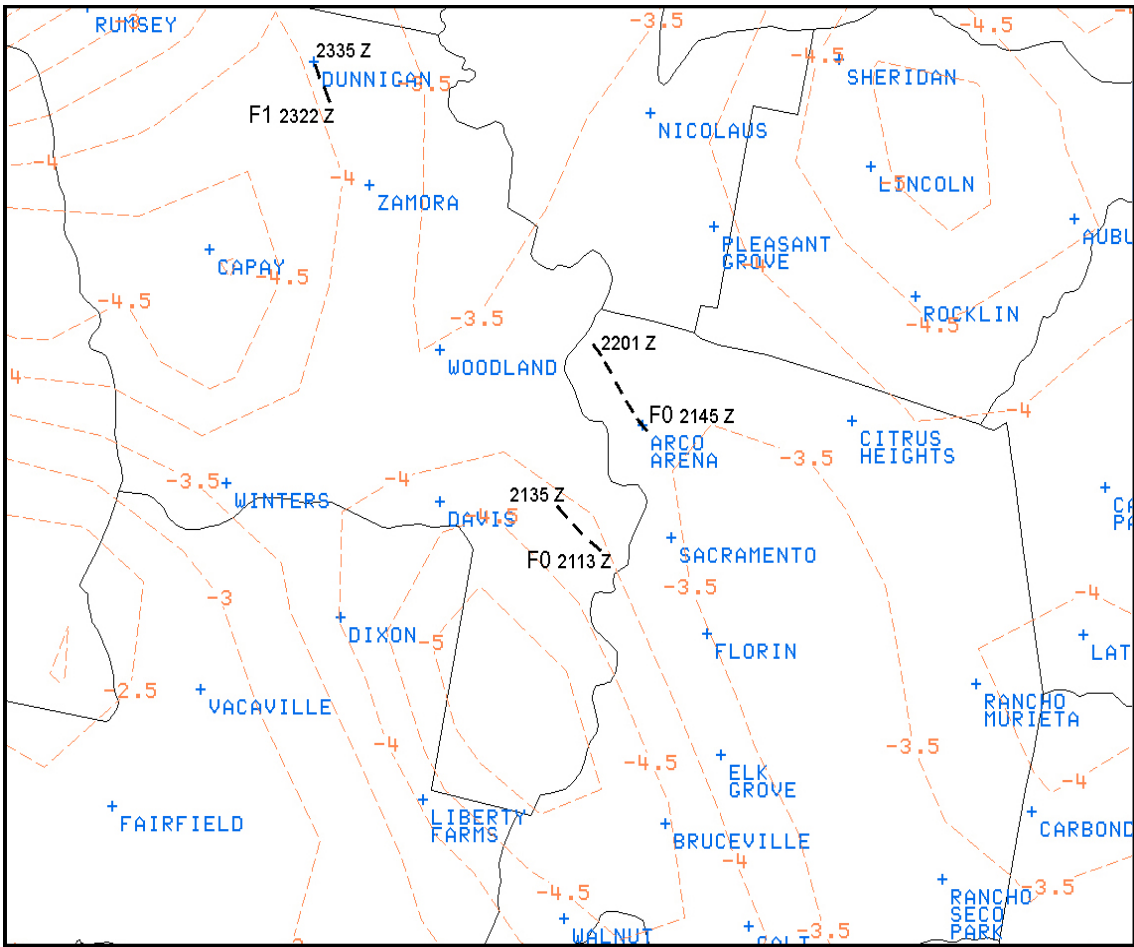


Figure 12a  
 2000Z 21 February 2005 LAPS Surface Computed Lifted Index (LI) with tornado  
 locations and times of occurrence (UTC). Note axis of most unstable air west of  
 Sacramento.

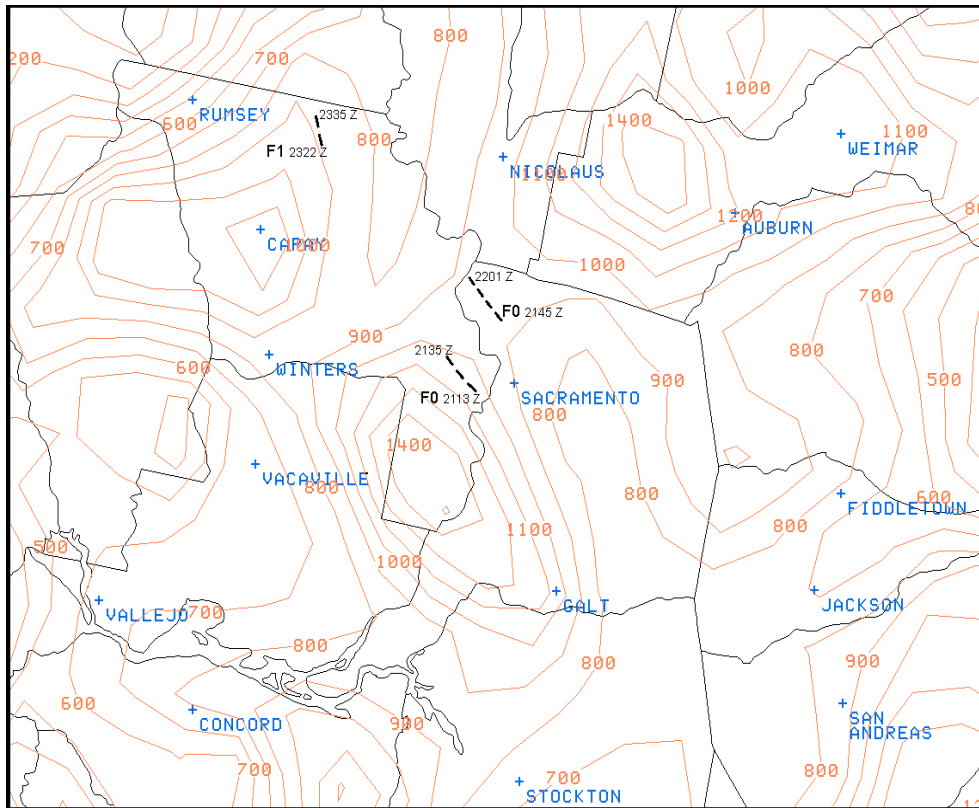


Figure 12b

2000Z 21 February 2005 LAPS CAPE (j/kg) with locations and times of occurrence (UTC). Note axis of largest values of CAPE west of Sacramento.

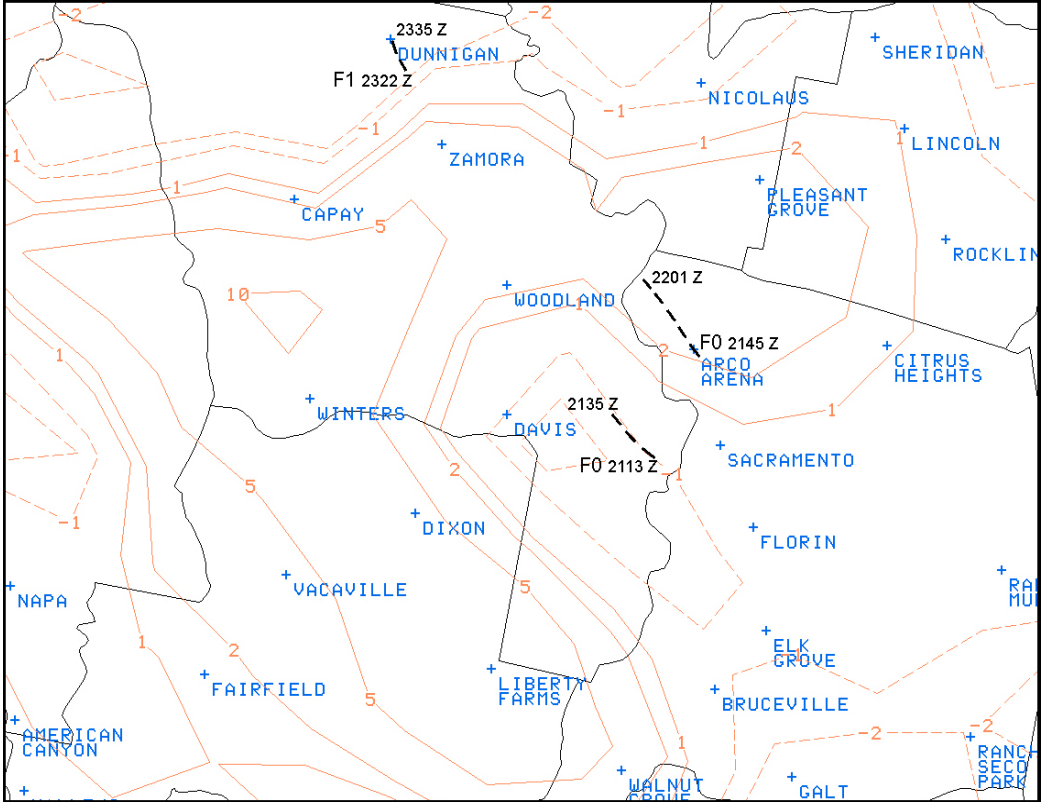


Figure 12c  
 2000Z 21 February 2005 LAPS Surface Moisture Advection (g/kg/12 hrs)  
 with tornado locations and times of occurrence (UTC). Note axis of surface  
 moisture advection west of Sacramento.

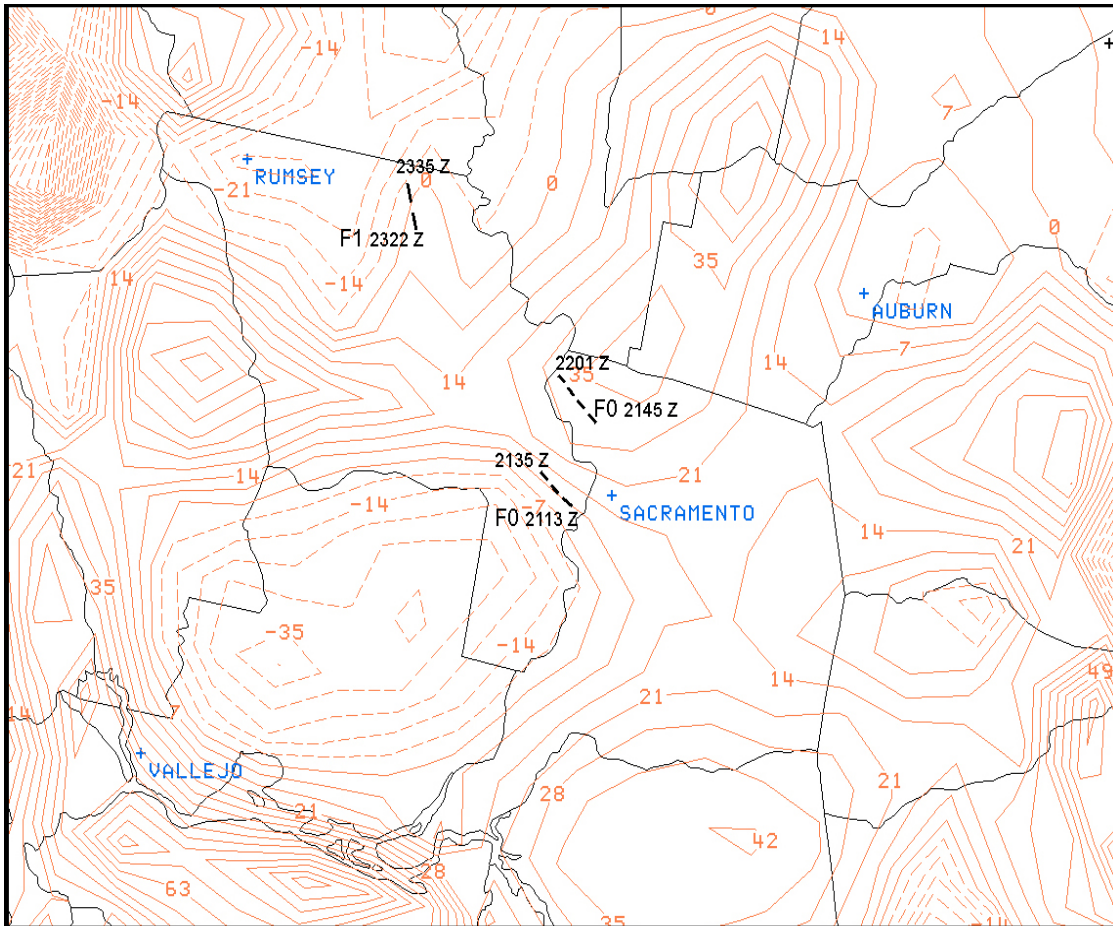


Figure 12d  
 2000Z 21 February 2005 LAPS Moisture Flux Divergence (g/kg/12 hrs) with  
 tornado locations and times of occurrence (UTC). Negative values indicate moisture  
 convergence and positive values moisture divergence. Note the gradient of values in  
 the vicinity and west of Sacramento.

### 3. RADAR IMAGERY

Radar imagery from the WSR-88D, Doppler radar located in Davis, CA (KDAX) was used to ascertain the time and location of the weather events on 21 February 2005. Radar analysis will be divided into 3 parts: the Southport, CA tornado, the Natomas, CA tornado, and the tornado near Dunnigan, CA.

All radar systems have inherent problems which make tornado detection difficult, and at times impossible. Smith (1996) and Burgess et al. (1993) discuss the problems of tornado detection by radar. Short-lived or very small circulations and vortices may go undetected due to the WSR-88D scan strategy, i.e. the time in between low level radar scans, distance from the radar, beam height, and beam resolution.

Because of the inherent limitations in radar data, forecasters need to closely monitor the storm environment. Brady and Szoke (1988) recommended using the WSR-88D reflectivity products to monitor the position and movement of low-level convergence boundaries, and to look for small circulations along boundaries that show continuity, develop and strengthen vertically, and are located near developing storms. Choy and Spratt (1994) used Echo Tops (ET), Vertically Integrated Liquid (VIL), and Composite Reflectivity (CR) products to observe rapid cell development along boundaries to detect waterspouts. Since the formation mechanism for waterspouts is similar for landspout tornadoes, forecasters can apply this technique to detect non-supercell tornadoes. Choy and Spratt (1994) did mention that this technique will not allow the forecaster to detect the circulation itself, and that the rotational signatures of these phenomena are often not resolvable by the WSR-88D.

The System for Convective Analysis and Nowcasting (SCAN) available with the Advanced Weather Information Processing System (AWIPS) Display Two Dimensions (D-2D) provides NWS forecasters the capability to monitor certain environmental parameters and attributes of individual thunderstorm cells. Although it does have its limitations (#), the cell table from SCAN allows forecasters to view trends of several parameters including maximum reflectivity, reflectivity height, VIL, hail size, etc., and displays alerts of a mesocyclone (MESO) and Tornado Vortex Signature (TVS) to assist forecasters in their warning decision making process.

Tornado detection in low-topped supercell tornadoes can also be a challenge, especially if the radar echoes are distant from the radar site and beam overshooting is apparent. Even with a low-topped supercell near the radar, the relative small circulation of the mesocyclone is not always easily identifiable as will be shown in subsequent sections.

(#) According to NOAA'S NWS Meteorological Development Laboratory (MDL) web page concerning the Severe Local Storm (svrwx) and Large Hail Algorithm (polh) "...the algorithms are intended primarily to alert forecasters to sudden or unexpected severe storm development. Other considerations, such as three-dimensional storm structure, storm motion, and real-time spotter reports must be used to decide which storms actually warrant warnings, and where the warnings should be valid."

However, monitoring the storm environment and applying the radar techniques of Brady and Szoke (1988), and Choy and Spratt (1994) may assist the forecaster in issuing more accurate and timely warnings.

## THE SOUTHPORT, CA TORNADO

Southport, CA is a small residential community located about 1.5 nautical miles (2.8 km) south of the city of West Sacramento, CA. An eyewitness stated that a tornado occurred between 2110Z and 2140Z (1:10 PM PST and 1:40 PM PST). Radar imagery suggests that this tornado probably occurred around 2113Z (1:13 PM PST).

Around 2100Z, KDAX radar detected two developing thunderstorms west and north of the Southport area. Notice from the 2113Z reflectivity data (Fig. 13a) that the thunderstorm cell was located west of the Southport area. Visible Satellite imagery and radar data suggested a flanking line of cumulus extended to the east-southeast of the parent thunderstorm. Given the timing and location of the tornado report, it is believed the Southport tornado developed along the flanking line (Fig. 13a) and in the proximity of the surface convergence boundary (Fig. 5b).

Storm Relative Velocity (SRM) data from the KDAX radar revealed a circulation at the 1.5 degree elevation at 2113Z along the flanking line and just south of West Sacramento over the Southport area (Figs. 13a and 13b). This circulation was evident on radar as it moved to the west-northwest through the 2135Z volume scan. Although the weak circulation associated with the tornado apparently crossed Interstate 80 west of the City of Sacramento it apparently did not do any significant damage after it briefly touched down in the Southport area. Damage to the Southport area was consistent with damage from a weak (F0) tornado. The damage path was approximately one-quarter to one-half mile in length and up to 300 yards wide. The damage was primarily to roofs of houses, although a large tree was toppled and several large tree branches fell on one residential property.

Radar imagery suggested the Southport tornado was the result of low level horizontal vorticity becoming tilted and stretched vertically along the flanking line. Markowski (et al. 1998) and Rasmussen (et al. 2000) discussed how low level horizontal vorticity along boundaries is an important vorticity source for low-level mesocyclones. It is believed the source of the horizontal vorticity for this storm was the surface boundary moving from the eastern portion of Sacramento County into the northwest portion of the county (Figs. 5a and 5b).

Radar indicated the Southport, CA tornado was misocyclonic. Fujita (1981) defined misocyclones as vortices in the horizontal plane with diameters less than 4 kilometers. The findings from the Southport, CA tornado follow the work of Lipari and Monteverdi (2000) who studied the soundings and hodographs of 30 northern and central California tornadic thunderstorms from 1990-1994 and concluded that most F0 events were misocyclonic. Marquis et al. (2004) noted that previous work on misocyclones by Wakimoto and Wilson (1989) discussed how misocyclones are often found along boundaries with horizontal shearing instability, including the leading edge of outflow boundaries from thunderstorms

(Fujita 1981, Mueller and Carbone 1987), cold fronts (Wilson 1986), drylines, and lines of convergence associated with wind shifts (Wilson et al., 1992 and Crook et al., 1991). Carbone (1982), Wilson (1986), Mueller and Carbone (1987), and Wakimoto and Wilson (1989) discussed how it is common for the radar reflectivity data to show ‘S’ shapes or whirls along the boundary where a mesocyclone is located, and how the strength of the rotation decreases with height. Figures 13a and 13b from the Southport, CA tornado certainly suggest the presence of mesocyclones along the boundary, although the reflectivity data do not indicate “S” shapes or whirls. This is most likely due to the fact that high resolution dual- and multi-Doppler radar observations were used in those studies compared to the observations from the KDAX WSR-88D used in the Southport, CA tornado.

The 2113Z KDAX 1.5 degree Storm Relative Motion (SRM) product indicated the strongest rotation at approximately 1100 feet MSL (~300 m), which then became broad and diffuse at subsequent higher elevation angles.

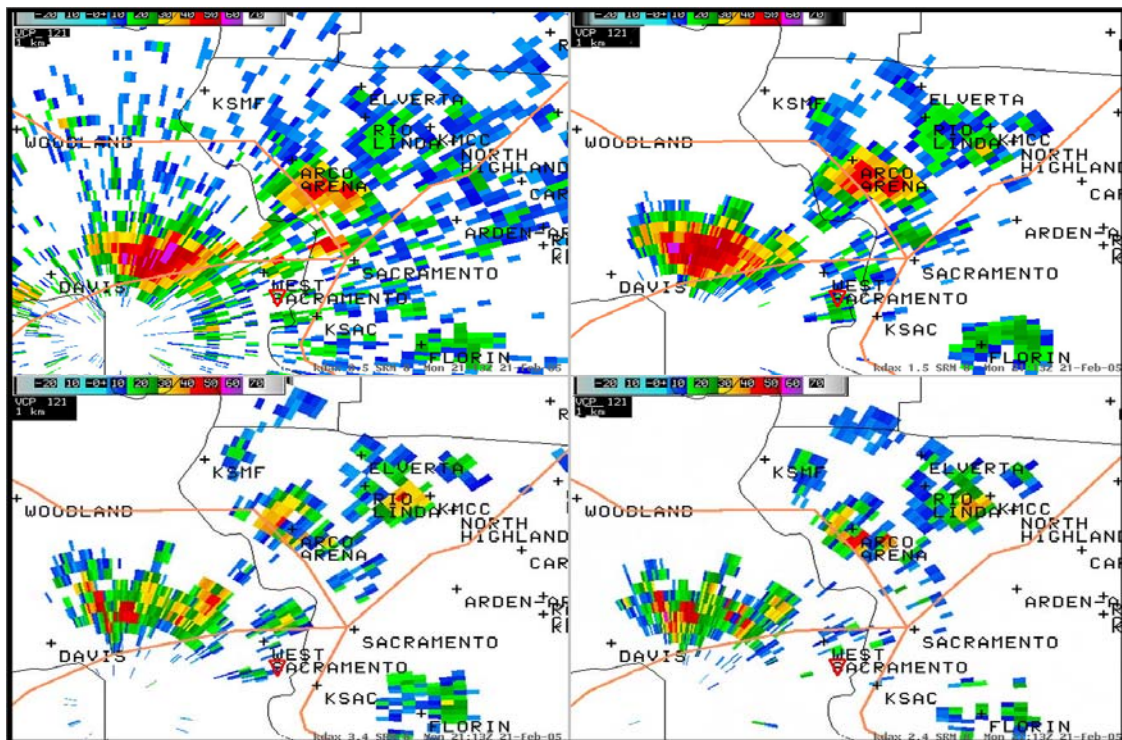


Figure 13a  
 WSR-88D Davis, CA (KDAX) 2113Z 21 February 2005 Base Reflectivity  
 Four Panel, 0.5 deg (UL), 1.5 deg (UR), 2.4 deg (LR), 3.4 deg (LL).  
 Inverted red triangle indicates tornado location.

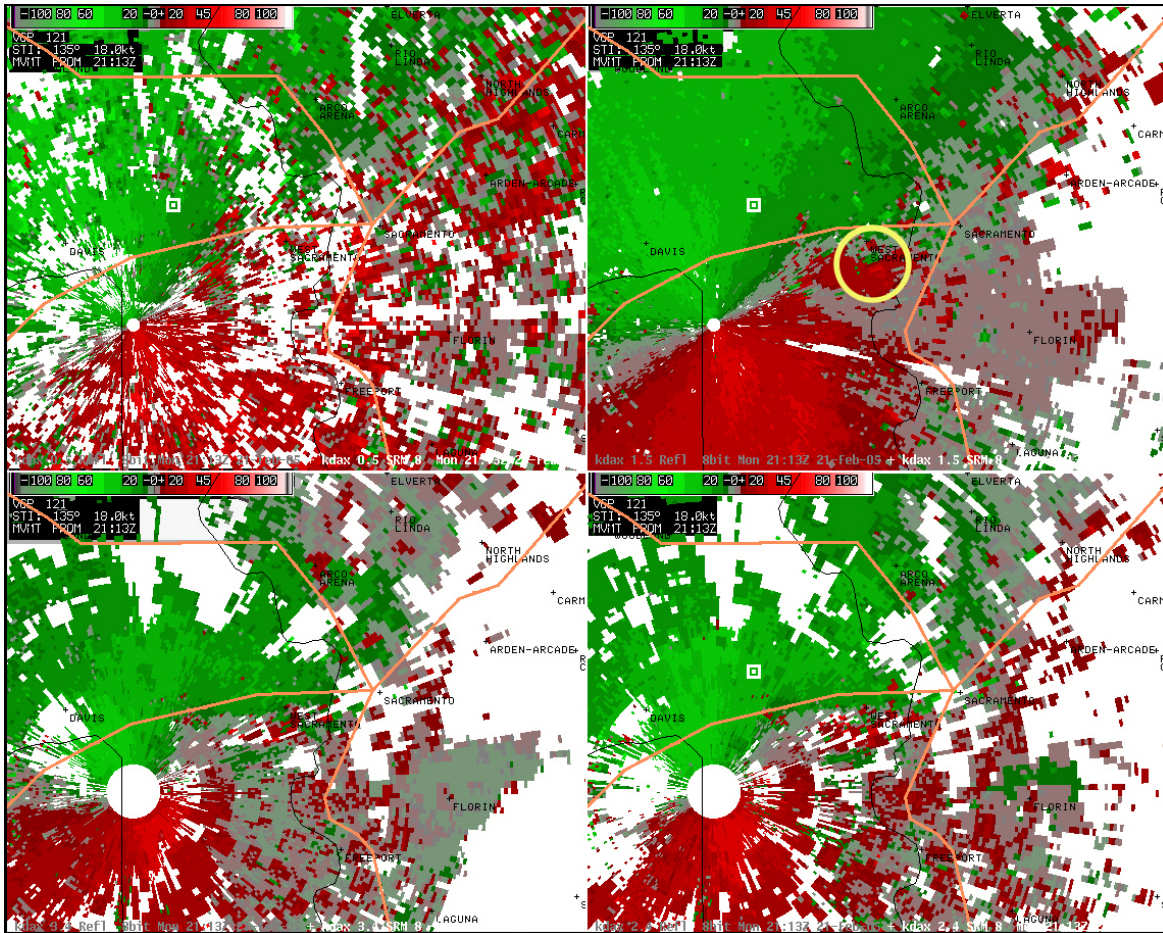


Figure 13b  
 WSR-88D Davis, CA (KDAX) 2113Z 21 February 2005 Storm Relative Motion (SRM) Four Panel, 0.5 deg (UL), 1.5 deg (UR), 2.4 deg (LR), 3.4 deg (LL). Yellow circle indicates circulation.

### THE NATOMAS, CA TORNADO

During and after the Southport, CA tornado, the thunderstorm to the northwest of Arco Arena (the Natomas area) intensified and reflectivity values approached 60 dBZ at 2129Z (2.4 degree elevation, 1950 feet MSL). The thunderstorm maintained its intensity as shown in the subsequent reflectivity volume scan in figure 14a. At 2135Z, Storm Relative Velocity (SRM) data showed a circulation just southeast of Arco Arena at the 1.5 degree, 2.4 degree and 3.4 degree elevation angles (Fig. 14b). This circulation moved to the west-northwest into northwest Sacramento County and towards Sacramento International Airport (KSMF) and dissipated by 2201Z. The 2145Z SRM 0.5 degree and 1.5 degree elevation angles indicated a circulation just east of Sacramento International Airport. The circulation was observed at 850 feet MSL at the 0.5 degree angle and at 2340 feet MSL at the 1.5 degree angle (Fig 15b).

Using the following equation to calculate rotational velocity ( $V_r$ ):

$$V_r = |V(\text{inbound}) + V(\text{outbound})|/2 \quad (1)$$

a rotational velocity of about 32 knots was observed between the maximum inbound and maximum outbound velocity couplet. Given the storm's distance from the KDAX radar and according to the 1.0 nautical mile nomogram from the WSR-88D Operational Support Facility (OSF) in Norman, OK, this would be characterized as a minimal mesocyclone.

This radar-indicated circulation is believed to have been the precursor to the tornado that struck the Natomas area (Figs. 15a and 15b). By 2155Z (1:55 PM PST), several severe weather reports from the Natomas area were relayed through the National Warning System (NAWAS) to the NWS Sacramento Forecast Office by the California Office of Emergency Services.

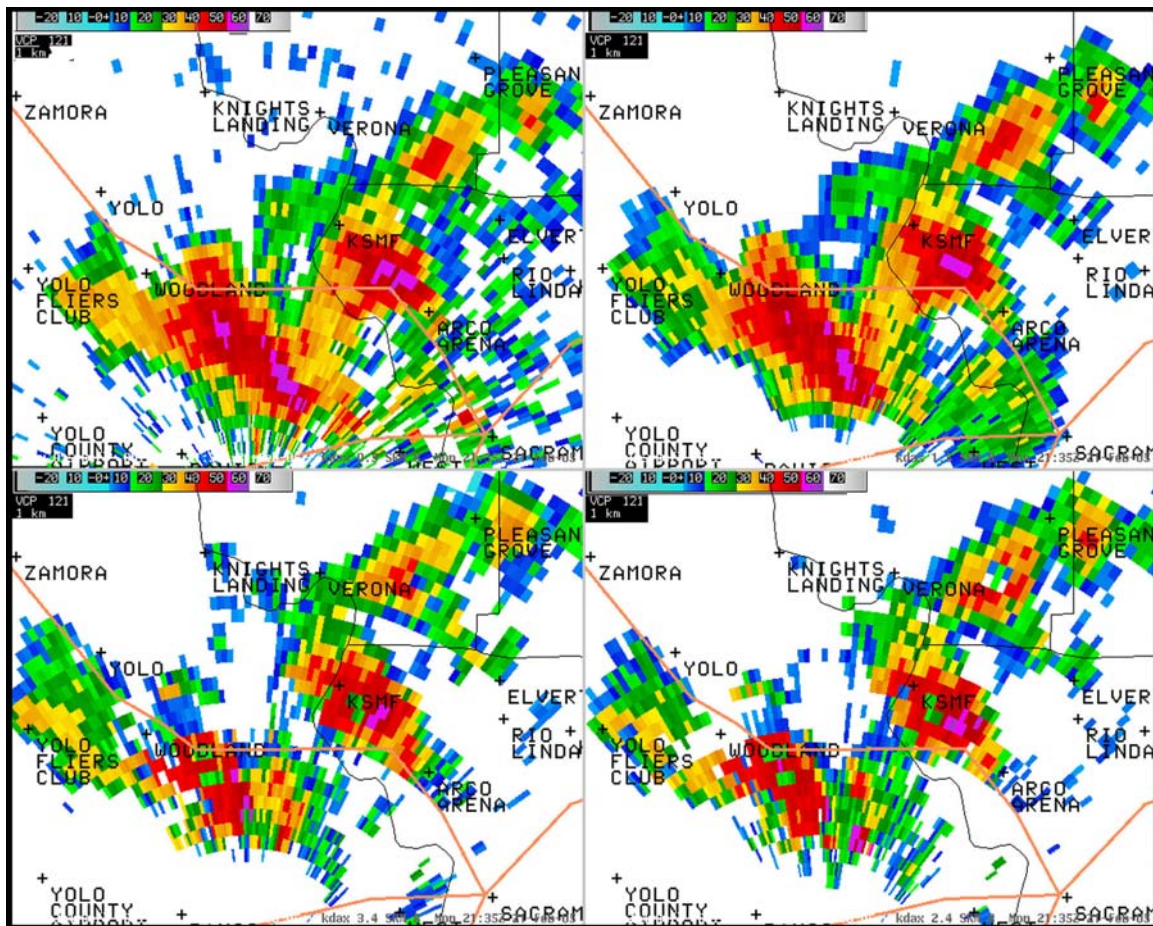


Figure 14a  
 WSR-88D Davis, CA (KDAX) 2135Z 21 February 2005 Base Reflectivity  
 Four Panel, 0.5 deg (UL), 1.5 deg (UR), 2.4 deg (LR), 3.4 deg (LL)

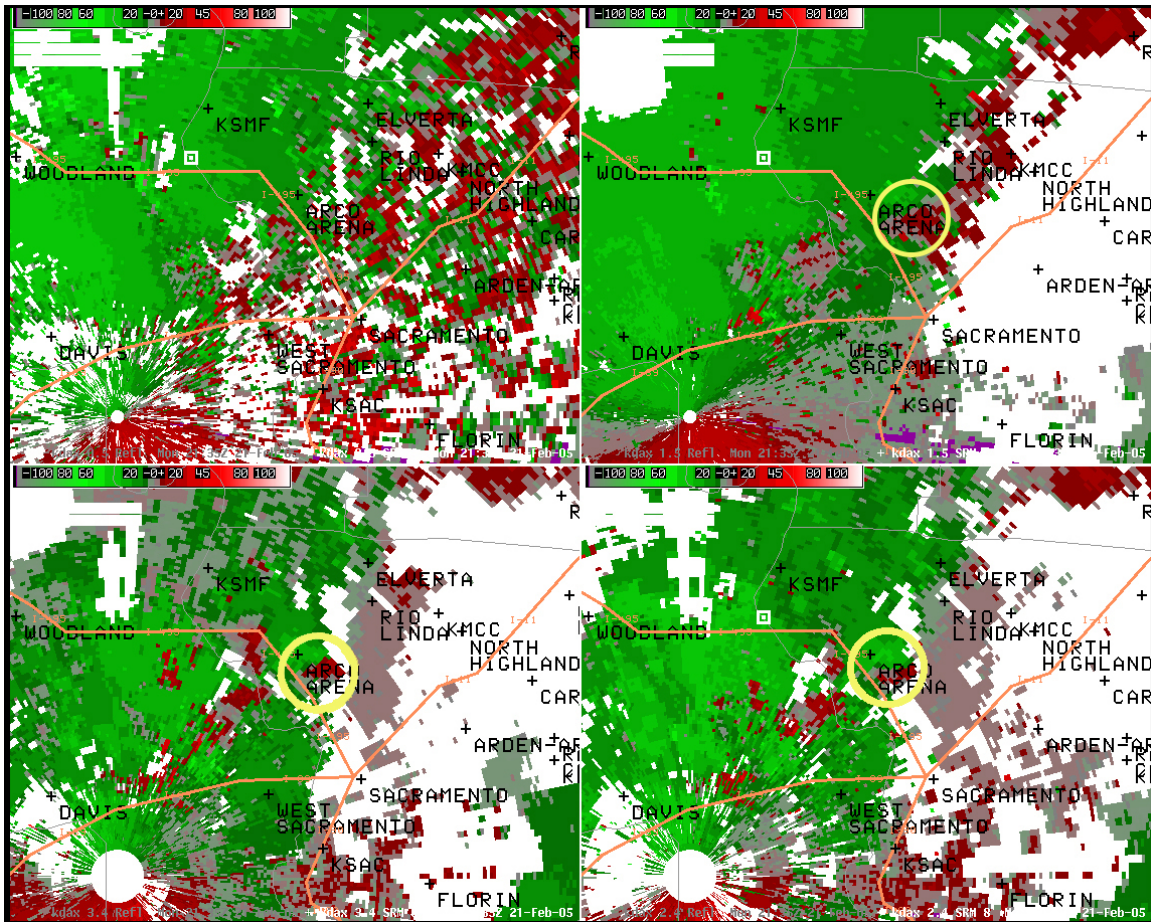


Figure 14b  
 WSR-88D Davis, CA (KDAX) 2135Z 21 February 2005 Storm Relative  
 Motion (SRM) Four Panel, 0.5 deg (UL), 1.5 deg (UR), 2.4 deg (LR),  
 3.4 deg (LL). Yellow circle indicates mesocyclone.

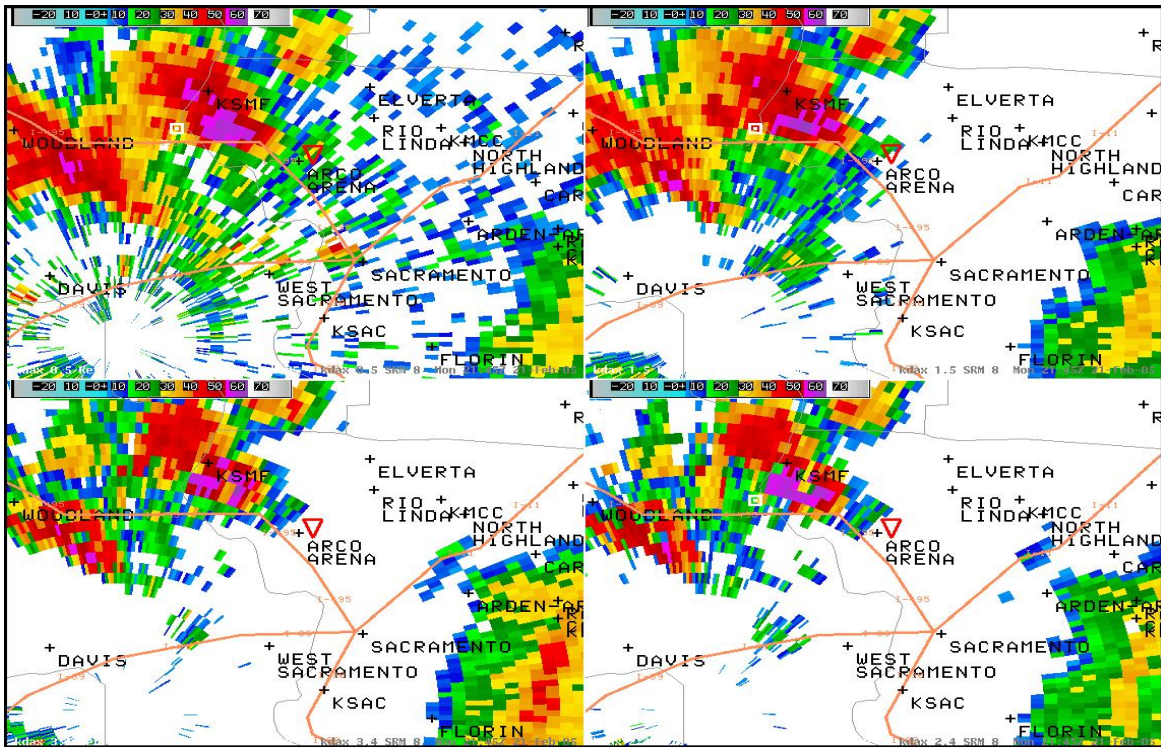


Figure 15a  
 WSR-88D Davis, CA (KDAX) 2145Z 21 February 2005 Base Reflectivity  
 Four Panel, 0.5 deg (UL), 1.5 deg (UR), 2.4 deg (LR), 3.4 deg (LL)  
 Inverted red triangle indicates tornado location.

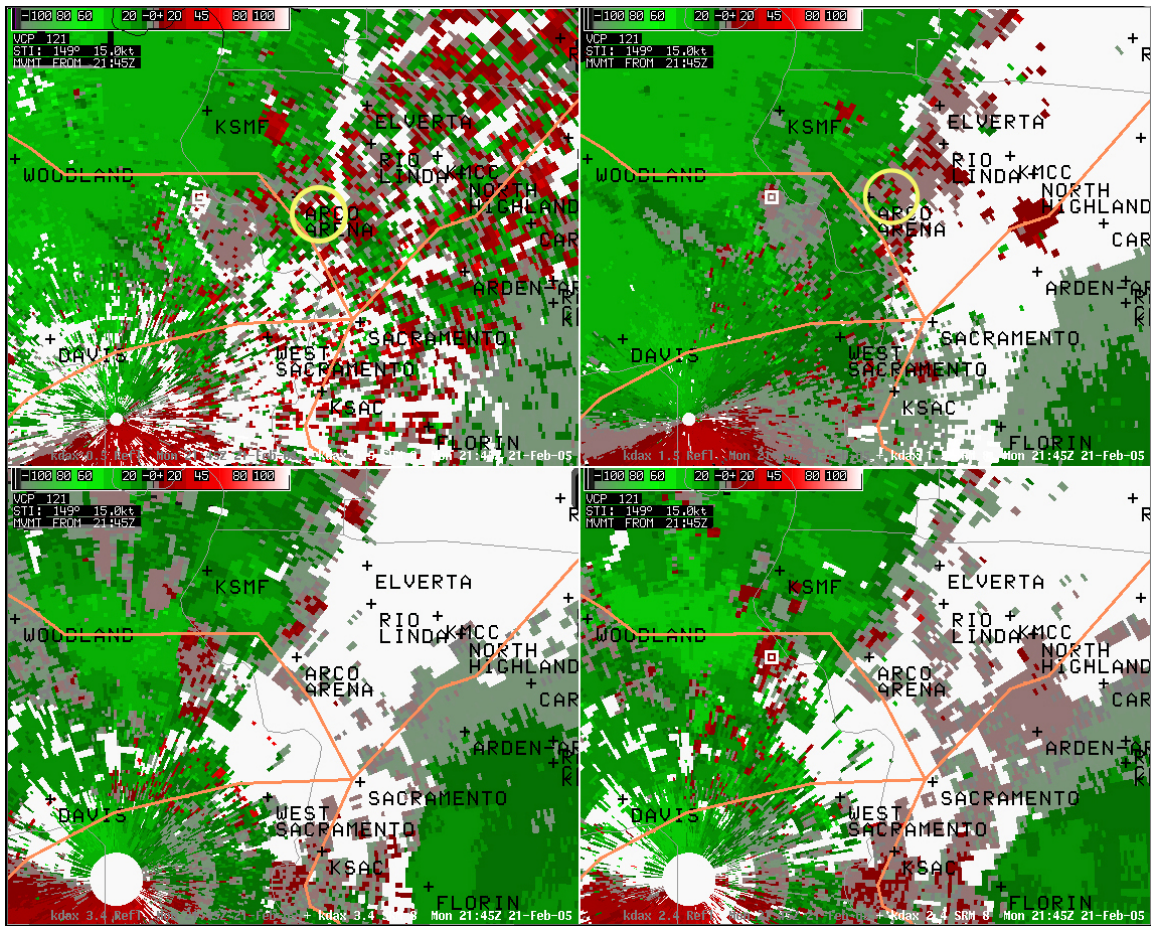


Figure 15b  
 WSR-88D Davis, CA (KDAX) 2145Z 21 February 2005 Storm Relative Motion (SRM) Four Panel, 0.5 deg (UL), 1.5 deg (UR), 2.4 deg (LR), 3.4 deg (LL). Yellow circle indicates mesocyclone.

The NWS issued a tornado warning for northwest Sacramento county, southeast Sutter county and northeast Yolo county at 2147Z based on available radar imagery, earlier public reports of funnel clouds in the area, and forecast thunderstorm movement. Though a tornado was confirmed a few minutes after the 2145Z radar imagery, the KDAX WSR-88D did not resolve an increase in rotational velocity associated with the circulation.

The Natomas tornado had a longer path length than the Southport tornado, about 1.5 miles to 2.0 miles long and up to 200 feet across. The damage path was also discontinuous and suggested that the tornadic circulation either ascended/descended several times, or wind speeds decreased sufficiently and minimized wind damage. A site survey of the damage indicated the most extensive damage occurred to a portion of a residential area north of North Park Drive. Most of the damage was to the terra-cotta roofing tiles on residential houses and wooded privacy fences. Along a walking path, a small area of natural grasses showed the evidence of a cyclonically rotating tornado.

Radar imagery suggested the Natomas tornado may have originated from the traditional “supercell cascade\*” process outlined by Wicker and Wilhelmson (1993). Typical for cool season California tornadic events the process from towering cumulus to a tornadic thunderstorm can occur relatively quickly, and in this case, took around one hour, from 2050Z to ~2155Z (12:50 PST to ~1:55 PM PST). This is characteristic of convective storms, rooted in the boundary layer, with steep lapse rates in a shallow layer under relatively low tropopause heights (Monteverdi et al. 2003). Storm Relative Velocity (SRM) data showed the development of the mid-level mesocyclone around 2135Z (1:35 PM PST, Fig. 14b), and then the development of the mesocyclone down to lower levels by 2145Z (1:45 PM PST, Fig. 15b), or about 10 minutes prior to the first report of a tornado.

The sequence of photographs of the Natomas tornado showed the characteristics of a tornado originating from the supercell cascade process (Figs. 16-19), rather than from a non-supercell. The photos (Figs. 16-19) indicate tornadogenesis occurred from the development of a mid-level mesocyclone and rear-flank downdraft (RFD), the lowering of the mesocyclone, and interaction of the RFD and low-level shear (note the curved inflow tail) to produce the tornado (Monteverdi et al. 2001). This is in contrast to the Southport, CA tornado where horizontal vorticity along a surface boundary was stretched and tilted upward by a rapidly developing thunderstorm updraft.

\*The supercell cascade leading to tornadogenesis is a conceptual model that starts with the development of the mid-level mesocyclone, advection of precipitation by the mesocyclone around the updraft area, development of a rear flank downdraft (RFD) simultaneous with the development of the mesocyclone at lower levels, and interaction of the RFD with the low-level shear to produce the low-level tornado cyclone and the eventual tornado. (From Monteverdi et al. 2001).



Figure 16

*Developing Natomas, CA tornado with Rear-Flank Downdraft (RFD) slot and base of wall cloud curving back to inflow tail. Looking west-northwest. Photo from Sacramento Bee newspaper.*



Figure 17

*Natomas, CA tornado showing the lowering of the rain free base, wall cloud and descending tornado. Lighter area on left side of photo indicative of Rear-Flank Downdraft (RFD) and lowering of mid-level mesocyclone to lower levels. Photo from Sacramento Bee newspaper.*



Figure 18

*Photo of mature tornado looking approximately 3 to 4 miles west of Natomas, CA towards Sacramento International Airport (KSMF) on 21 February 2005. Photo by Rob Cernohlavek. From Sacramento Bee Newspaper.*



Figure 19

*Natomas, CA tornado during dissipating or rope stage near Sacramento International Airport (KSMF). Photo from Sacramento Bee newspaper.*

The persistent mesocyclone in the lower- to mid-levels of a thunderstorm differentiates a supercell from an ordinary thunderstorm. Supercells have disparate storm motions due to the effect of the horizontal updraft-shear propagation component that is perpendicular to the shear vector, and parallel to the horizontal vorticity vector for left-moving supercells, and anti-parallel to the horizontal vorticity for right-moving supercells (Zeitler and Bunkers 2005). Bunkers et al. (2000) developed a hodograph technique to predict supercell motion. Applying Bunkers technique to the Natomas, CA tornadic storm for a vertical wind shear profile in the upper-left quadrant of the hodograph, a cyclonic supercell would move left of the mean wind (and slower) even though this would still be to the right of the vertical wind shear vector (Bunkers et al. 2000) (see hodograph, Fig. 20).

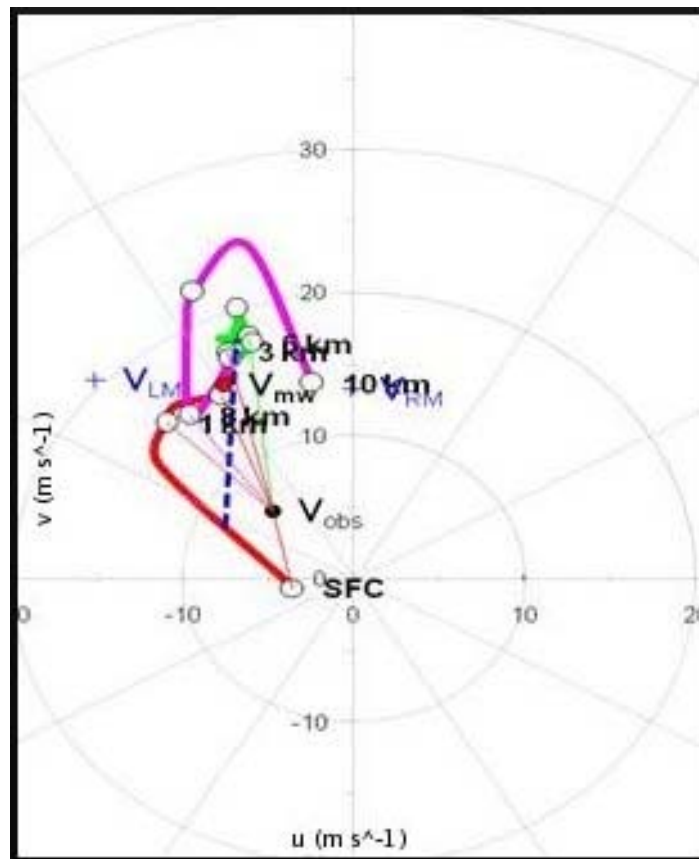


Figure 20

*Hodograph for the Natomas, CA supercell using the KOAK Oakland, CA 12Z 21 February 2005 sounding.  $V_{RM}$  ( $V_{LM}$ ) is the predicted right-moving (left-moving) supercell motion from Bunkers et al. (2000).  $V_{obs}$  is the observed supercell motion (from 135 degrees at  $6.7 \text{ m s}^{-1}$  or 13 kts). Dashed line represents surface to 6 km shear.  $V_{mw}$  (red circle) is the surface to 6 km mean wind. Units are meters/second.*

It is interesting to note that Bunkers method did not predict the right-moving supercell motion very well. This may be due to the fact that the hodograph plot was based on radiosonde data from the nearest upper air site, Oakland, CA (KOAK). Radiosonde data have two substantial limitations with respect to forecasting severe convection, i.e. poor temporal and spatial resolution (Bunkers et al. 2000). However, an effort was made to quality control the radiosonde data by using the WSR-88D Davis, CA (KDAX) VAD Wind Profile (VWP). It is worth noting that the observed storm motion was ideal for the ingestion of storm relative helicity (Figs. 21a-21c).

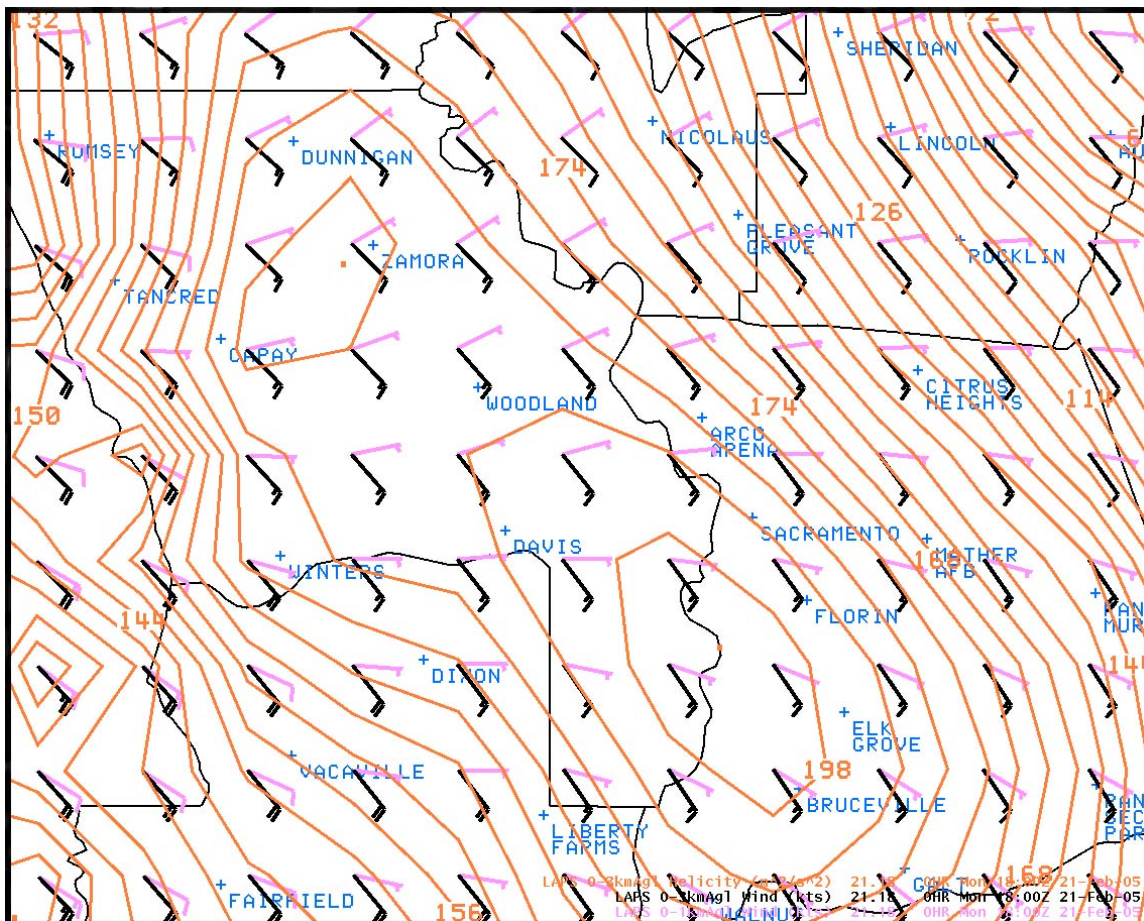


Figure 21a  
 1800Z 21 February 2005 LAPS 0-3 km Helicity,  $m^2/s^2$ , (orange),  
 LAPS 0-1 km AGL Wind (magenta), and LAPS 0-3 km AGL Wind (black).

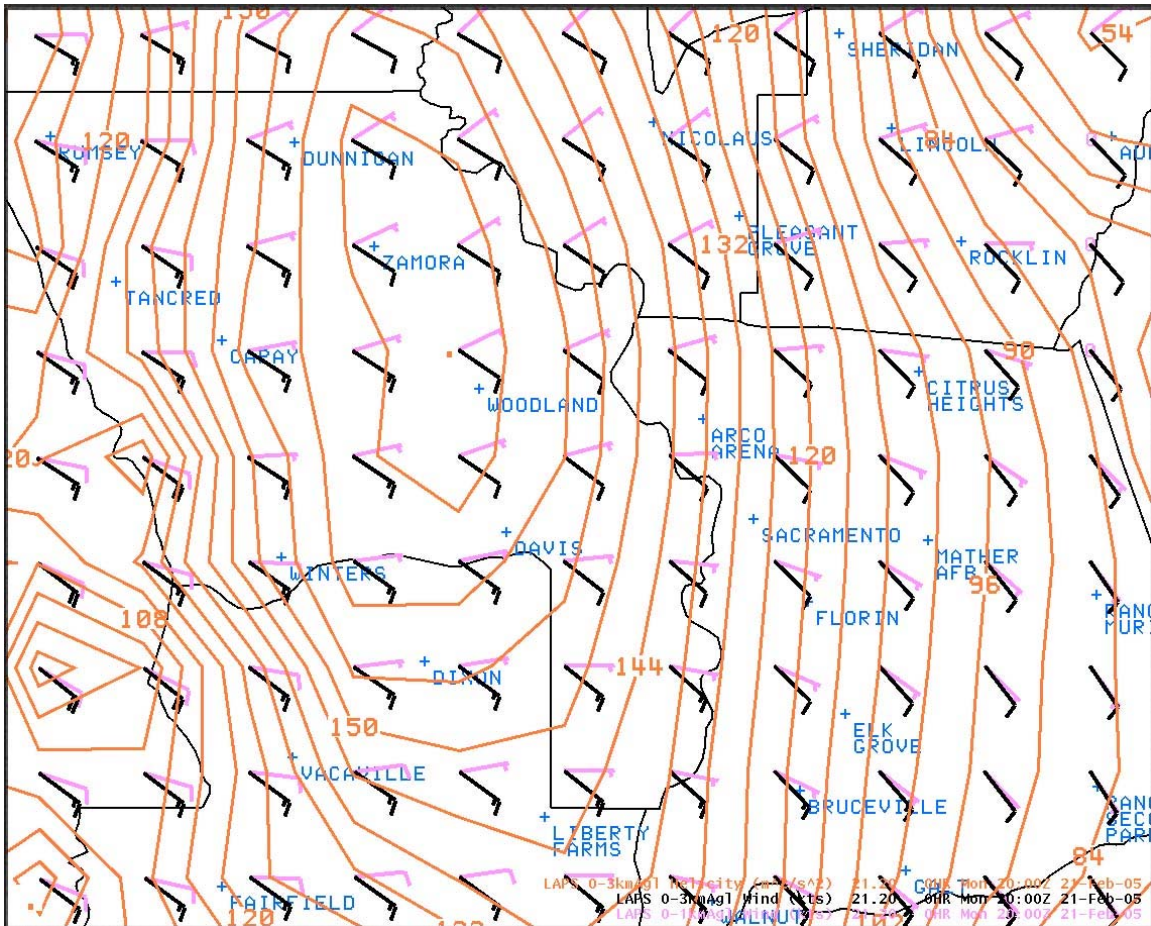


Figure 21b  
 2000Z 21 February 2005 LAPS 0-3 km Helicity, m<sup>2</sup>/s<sup>2</sup>, (orange),  
 LAPS 0-1 km AGL Wind (magenta), and LAPS 0-3 km AGL Wind (black).

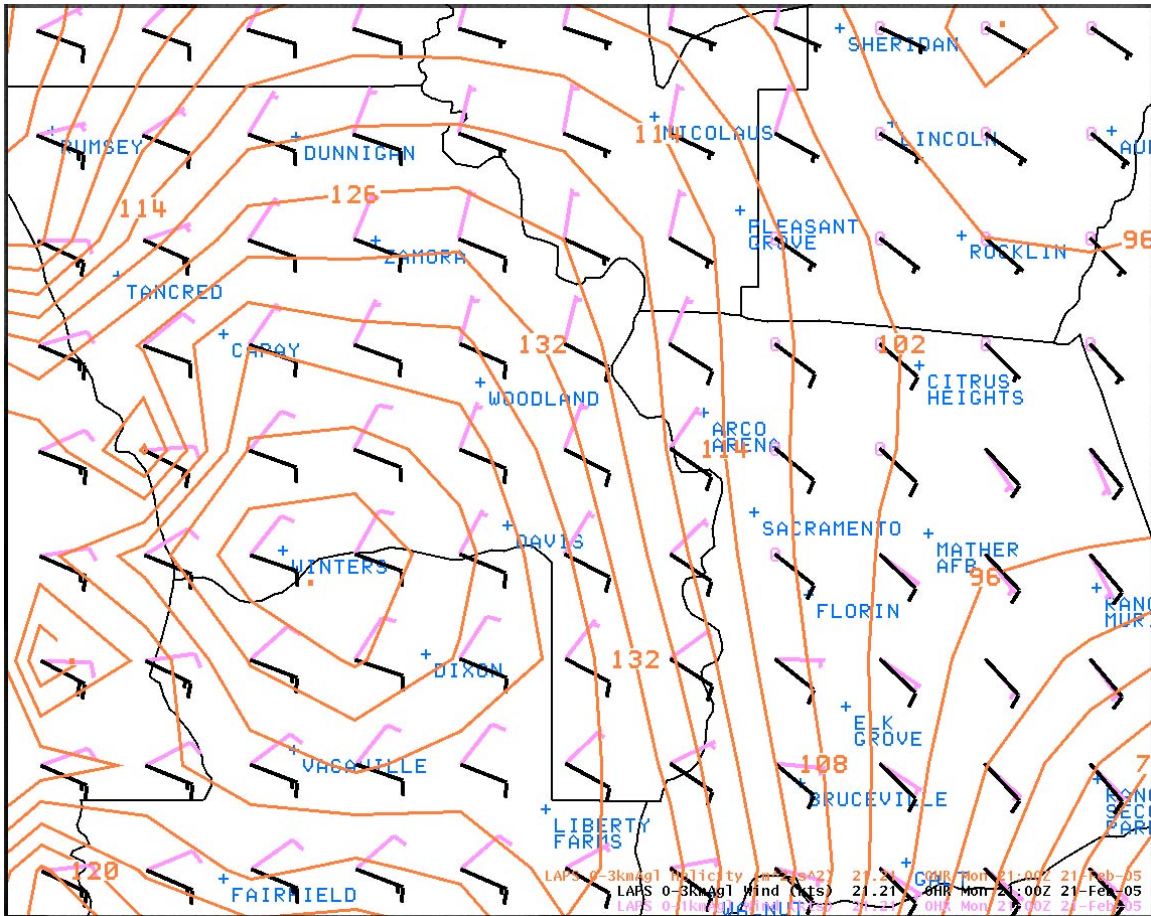


Figure 21c  
 2100Z 21 February 2005 LAPS 0-3 km Helicity,  $m^2/s^2$ , (orange),  
 LAPS 0-1 km AGL Wind (magenta), and LAPS 0-3 km AGL Wind (black).

The hodograph in figure 20 was rotated clockwise 90 degrees to illustrate the similarity to the composite hodographs for F1/F2 tornadoes in figure 11. Note the hodographs have marked anticyclonic loops that are typical for tornadic storms in northern and central California (Fig. 22).

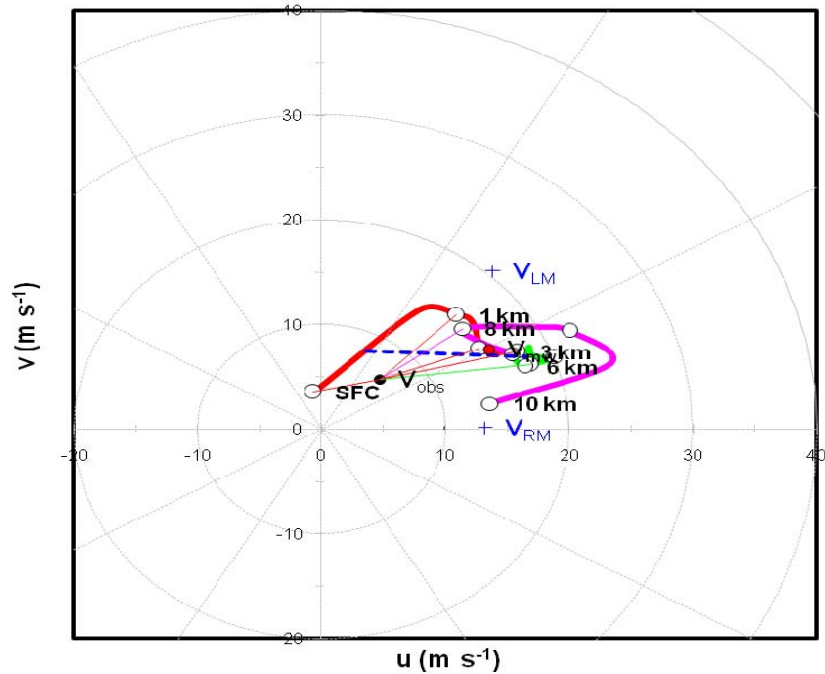


Figure 22

*Hodograph for the Natomas, CA supercell, rotated clockwise 90 degrees, using the KOAK Oakland, CA 12Z 21 February 2005 sounding.  $V_{RM}$  ( $V_{LM}$ ) is the predicted right-moving (left-moving) supercell motion from Bunkers et al. (2000).  $V_{obs}$  is the observed supercell motion. Dashed line represents surface to 6 km shear.  $V_{mw}$  (red circle) is the surface to 6 km mean wind. Units are meters/second.*

## THE DUNNIGAN, CA TORNADO

Other than radar and photographic evidence (Fig. 23) very little is known about the Dunnigan, CA tornado. The tornado occurred in a very rural area, and consequently, there were no damage reports relayed to the Sacramento NWS Office.



Figure 23  
*Photo of tornado near Dunnigan, CA on 21 February 2005.  
Photo from Sacramento Bee newspaper.*

Radar imagery indicated a weakening of the circulation of the Natomas tornado after 2201Z (2:01 PM PST). However, two thunderstorms (marked “A” and “B” in Fig. 24a) began to merge between Knights Landing and Yolo from 2217Z and 2227Z (2:17 PM and 2:27 PM PST) as they moved into the more unstable environment (Figs. 12-12d). Thunderstorm intensity increased with reflectivity values over 60 dBz at the 0.5 degree, 1.5 degree, and 2.4 degree elevations (1126 to 4670 feet MSL) as cell “B” neared Knight’s Landing. Even though cell “B” had the highest reflectivity of the two cells, cell “A” to the east southeast of Yolo, CA exhibited BWER, hook echo, and mesocyclone features that did not exist in cell “B” (Figs. 24a and 24b). Also, divergence in the 0.5 degree SRM suggested weak outflow along the southern flank of cell “B”.

With the initial tornado warning about to expire, the WFO forecaster had to make a new warning decision. Without the benefit of additional real-time tornado reports after the Natomas and Southport tornadoes, it was uncertain if a tornado was still occurring. Lindsey and Bunkers (2005) discussed storm interaction and how tornadic storms can cease producing tornadoes during and immediately after cell merger, but then reorganize and re-intensify to produce additional strong tornadoes at a later time. The decision was made to issue a severe thunderstorm warning, and mention in the text that “*Severe thunderstorms can also produce tornadoes*” to heighten public awareness. This warning was followed with another severe thunderstorm warning with similar wording as the storm moved closer to Dunnigan, CA.

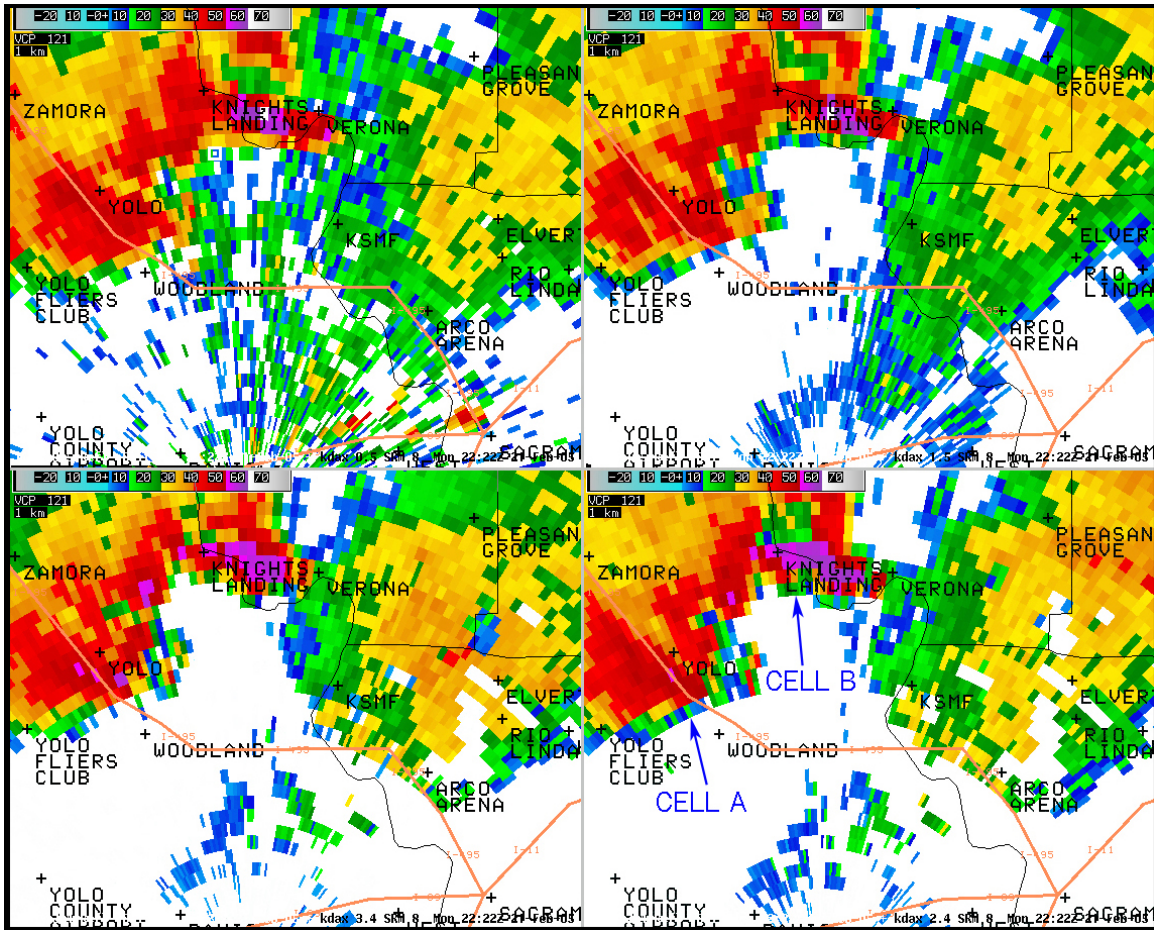


Figure 24a  
 WSR-88D Davis, CA (KDAX) 2222Z 21 February 2005 Base Reflectivity  
 Four Panel, 0.5 deg (UL), 1.5 deg (UR), 2.4 deg (LR), 3.4 deg (LL). Note  
 location of cells "A" and "B" in lower right panel.

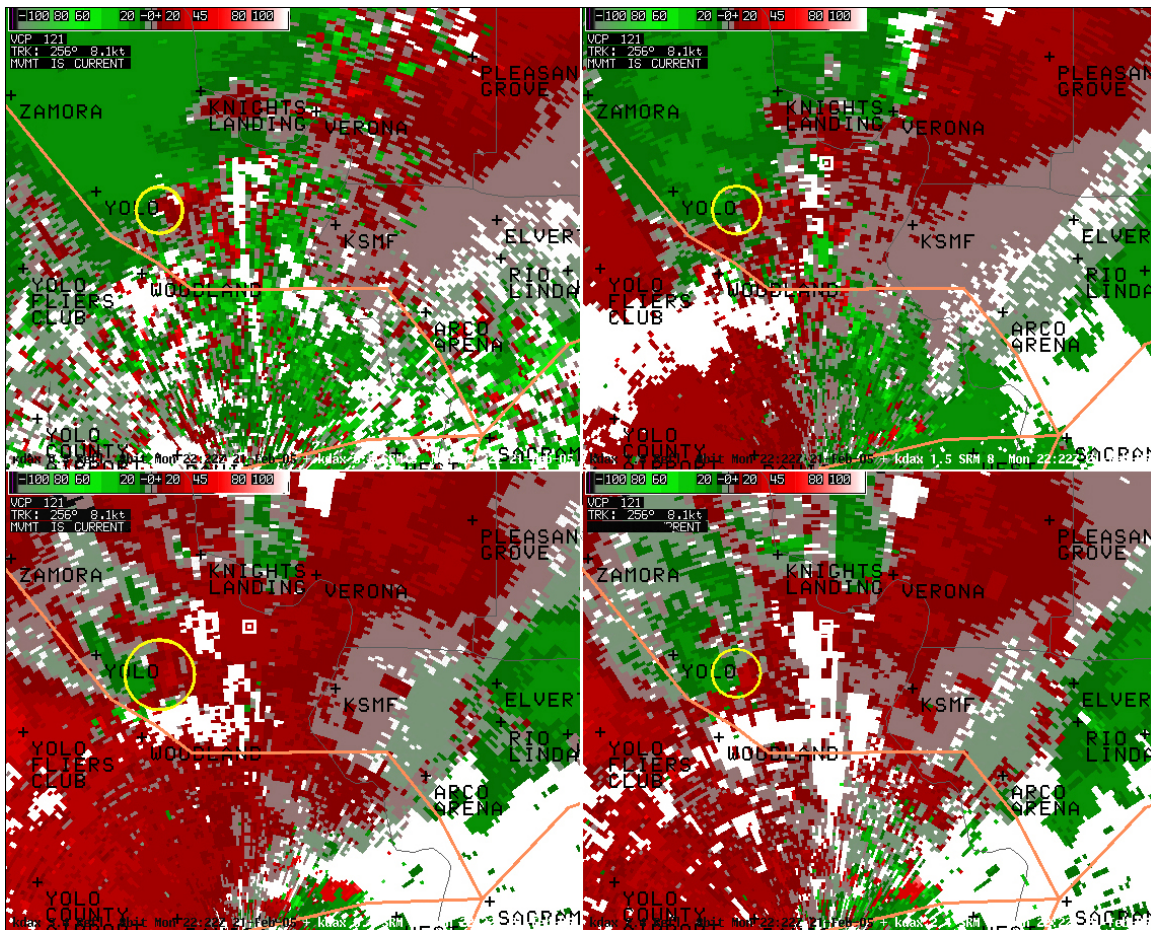


Figure 24b  
 WSR-88D Davis, CA (KDAX) 2222Z 21 February 2005 Storm Relative Motion (SRM) Four Panel, 0.5 deg (UL), 1.3 deg (UR), 2.4 deg (LR), 3.1 deg (LL). Yellow circle indicates mesocyclone.

Animation of the radar imagery indicated the storm motion of the thunderstorm cells backed slightly from the initial storm motion of 135 degrees at 13 knots, to 125 degrees at 12 knots as the merged storm approached Dunnigan, CA from the east. This may have been the result of deviant supercell storm motion discussed by Zeitler and Bunkers (2005), or the rotation from the mid- and upper-level vorticity maximum discussed earlier. Animation of the KDAX VAD Wind Profiler (VWP) showed a subtle backing of the lower- to mid-level winds (approximately 5,000 to 26,000 feet MSL) about 30 minutes prior to the Dunnigan, CA tornado before there was a lack of detectable echoes on the VWP after 2248Z.

The southern flank of the merged cell is the suspected area for tornadogenesis. This is due to the more unstable environment (Figs. 12a-12d), and the higher helicity values (Figs. 21a-21c) to the south. It is likely the storm ingested more streamwise vorticity which led to reorganization and re-intensification of the storm and an additional, possibly stronger, tornado. Applying Bunkers technique to the Dunnigan, CA tornadic storm for a vertical

wind shear profile in the upper-left quadrant of the hodograph, a cyclonic supercell would move left of the mean wind (and slower) even though this would still be to the right of the vertical wind shear (Bunkers et al. 2000) (see hodograph, Fig. 25). The observed storm motion was ideal for the ingestion of storm relative helicity (Figs. 21a-21c).

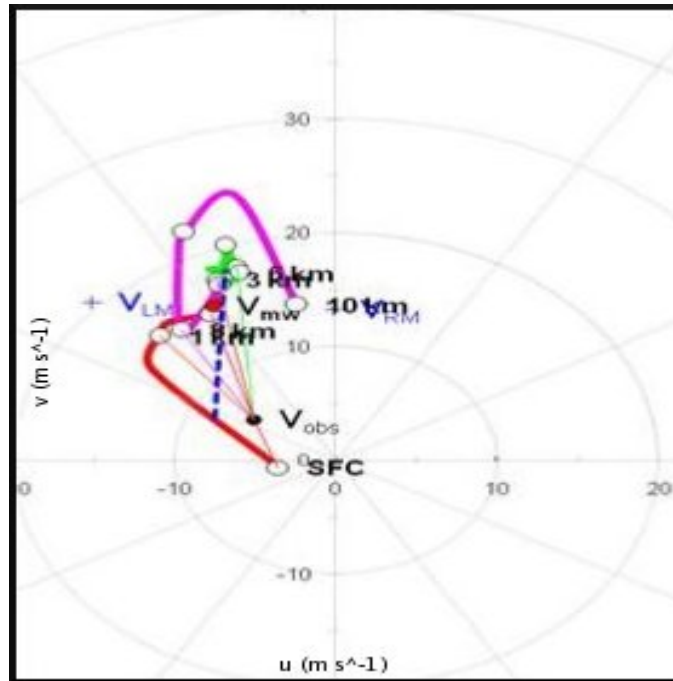


Figure 25

*Hodograph for the Dunnigan, CA supercell using the KOAK Oakland, CA 12Z 21 February 2005 sounding.  $V_{RM}$  ( $V_{LM}$ ) is the predicted right-moving (left-moving) supercell motion from Bunkers et al. (2000).  $V_{obs}$  is the observed supercell motion (from 125 degrees at  $6.2 \text{ m s}^{-1}$  or 12 kts). Dashed line represents surface to 6 km shear.  $V_{mw}$  (red circle) is the surface to 6 km mean wind. Units are meters/second.*

At 2310Z (3:10 PM PST), thunderstorm cell intensity increased to 60.5 dBZ about 3 nautical miles east-northeast of Dunnigan at the 1.3 degree elevation angle (4050 feet MSL, figure not shown). At this time, the Storm Relative Motion (SRM) 2.4 and 3.1 degree elevation angles revealed a weak or minimal mesocyclone between 6000 feet and 7700 feet MSL (figures not shown). It is difficult to determine if the circulation reached the ground, but it is believed that it did not due to the lack of reports of tornado sightings in close proximity to heavily traveled Interstate 5.

The SRM data show the mesocyclone lowering to the 1.3 degree elevation angle (Fig. 26b) at 2314Z (3:14 PM PST), and lowering to the 0.5 SRM elevation angle, approximately

1650 feet MSL, at 2322Z (3:22 PM PST, Fig. 27b). Using the following equation to calculate rotational velocity ( $V_r$ ):

$$V_r = |V(\text{inbound}) + V(\text{outbound})|/2 \quad (2)$$

a rotational velocity of about 50 knots was observed between the maximum inbound and maximum outbound velocity couplet. Given the storm's distance from the KDAX radar and according to the 1.0 nautical mile nomogram from the WSR-88D Operational Support Facility (OSF) in Norman, OK, this would be characterized as a strong mesocyclone. Note on the corresponding reflectivity products (Figs. 26a and 27a) the location of the hook echo and/or tornado location relative to the storm.

The mesocyclone was evident at the knob-end of the reflectivity hook echo just east of Dunnigan, CA at 2331Z (3:31 PM PST, Figs. 28a and 28b). Based on the radar evidence, it is believed the Dunnigan tornado occurred from around 2322Z (3:22 PM PST) to around 2335Z (3:35 PM PST). It is believed the photograph in Figure 23 was also taken within that time.

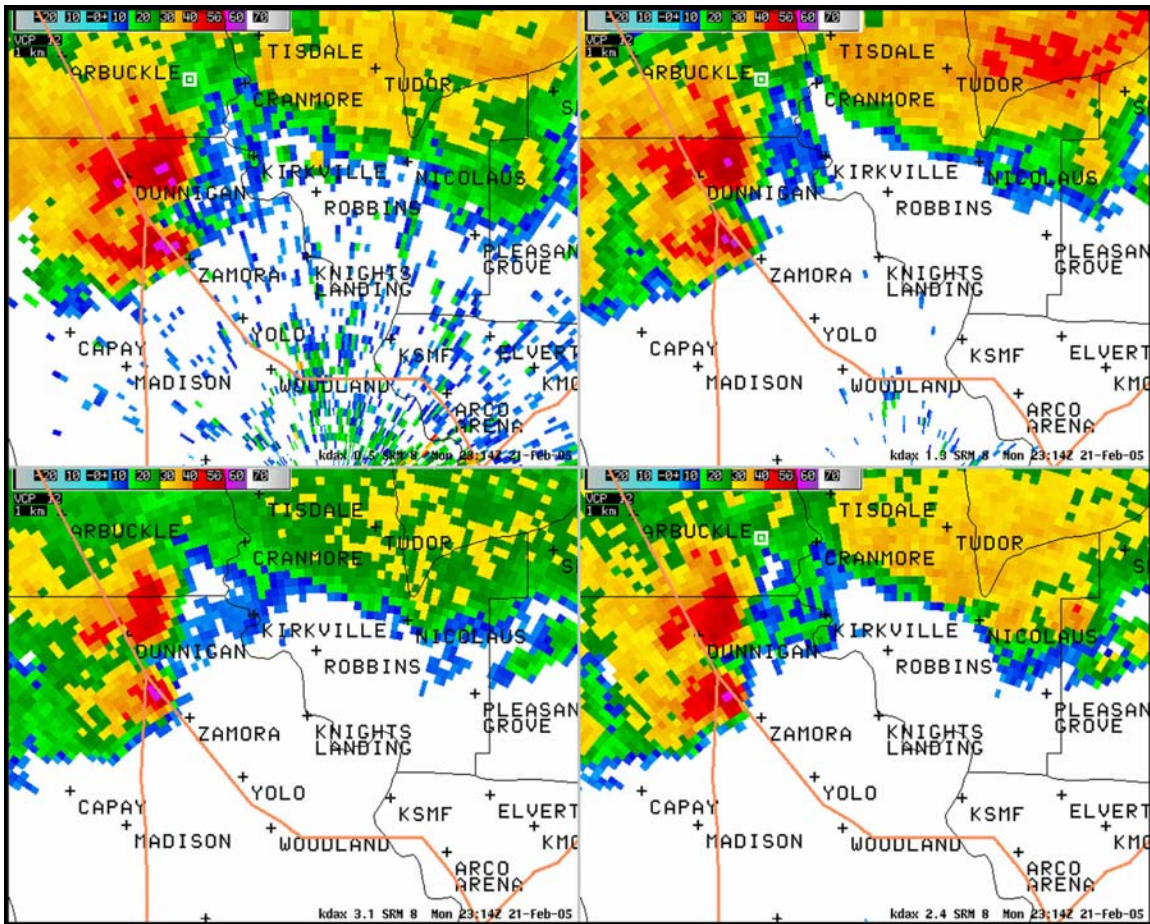


Figure 26a  
 WSR-88D Davis, CA (KDAX) 2314Z 21 February 2005 Base Reflectivity  
 Four Panel, 0.5 deg (UL), 1.3 deg (UR), 2.4 deg (LR), 3.1 deg (LL).

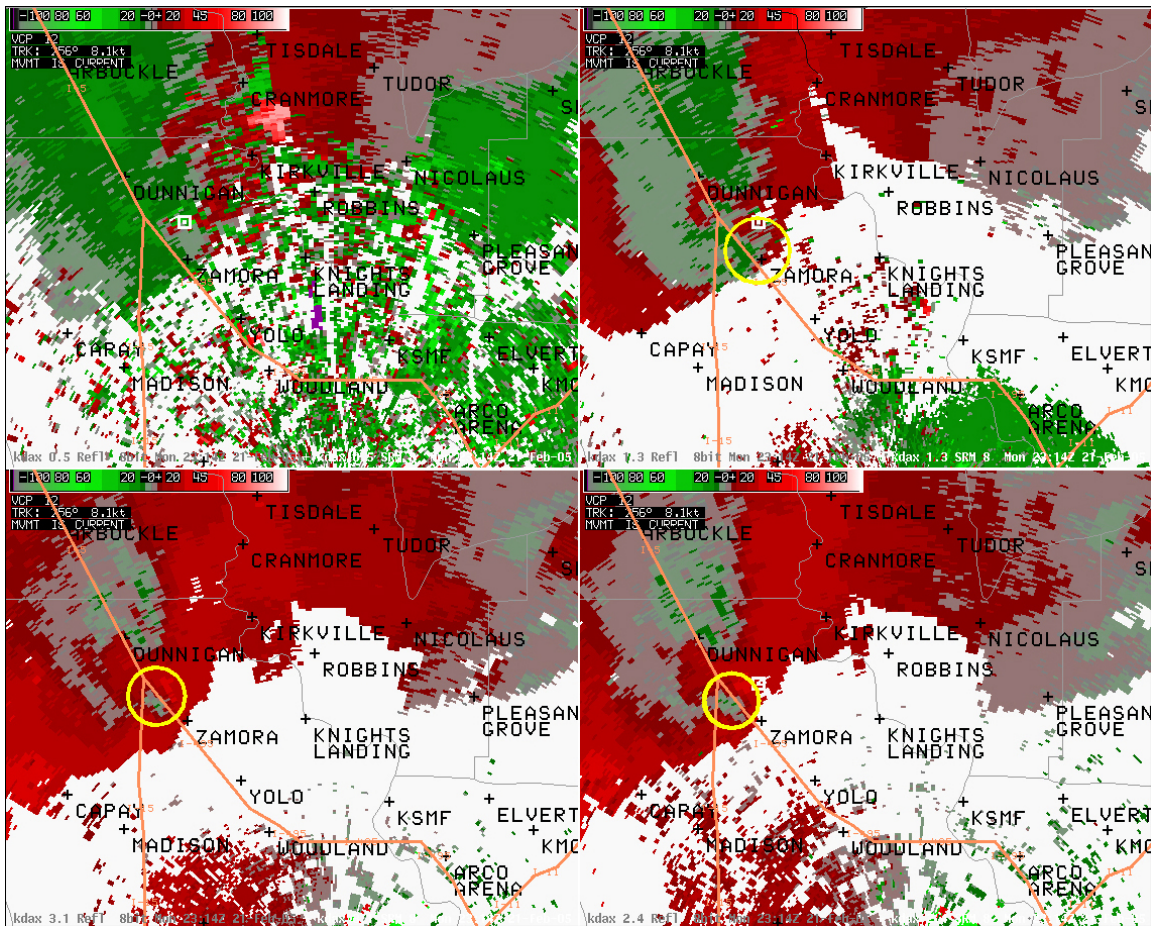


Figure 26b  
 WSR-88D Davis, CA (KDAX) 2314Z 21 February 2005 Storm Relative  
 Motion (SRM) Four Panel, 0.5 deg (UL), 1.3 deg (UR), 2.4 deg (LR),  
 3.1 deg (LL). Yellow circle indicates mesocyclone.

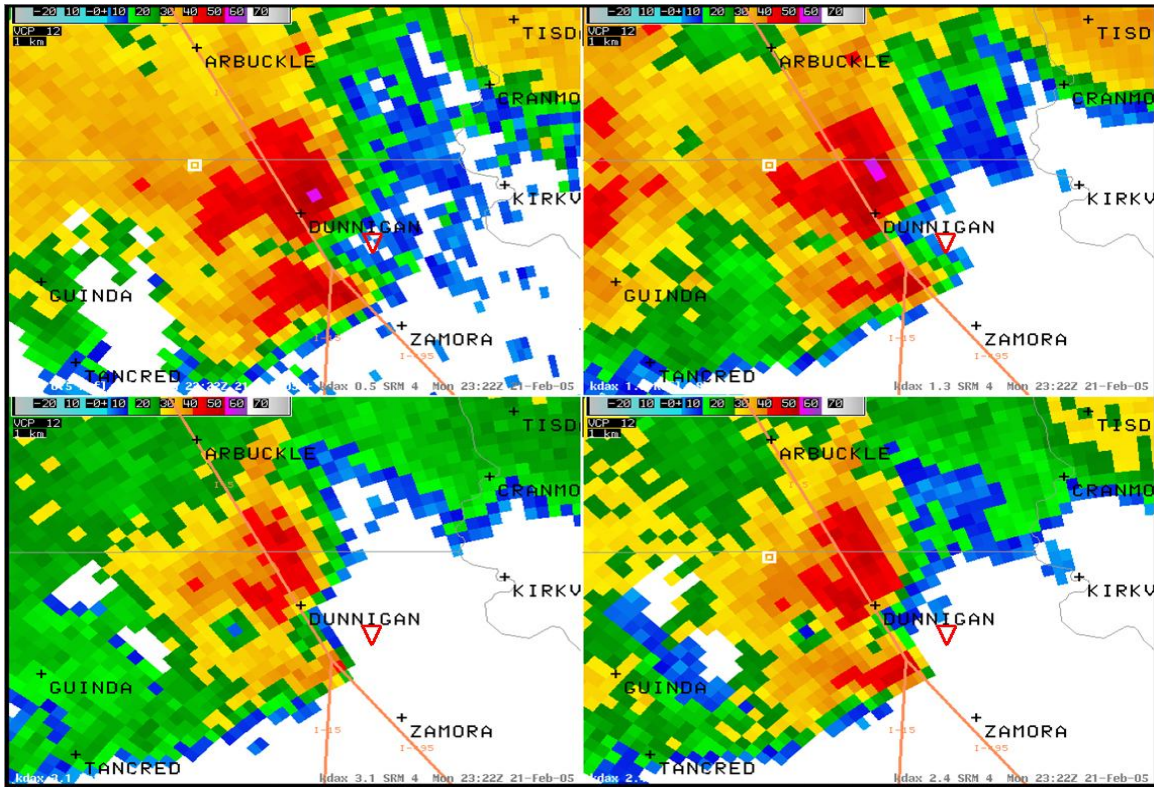


Figure 27a  
 WSR-88D Davis, CA (KDAX) 2322Z 21 February 2005 Base Reflectivity  
 Four Panel, 0.5 deg (UL), 1.3 deg (UR), 2.4 deg (LR), 3.1 deg (LL)  
 Inverted red triangle indicates tornado location.

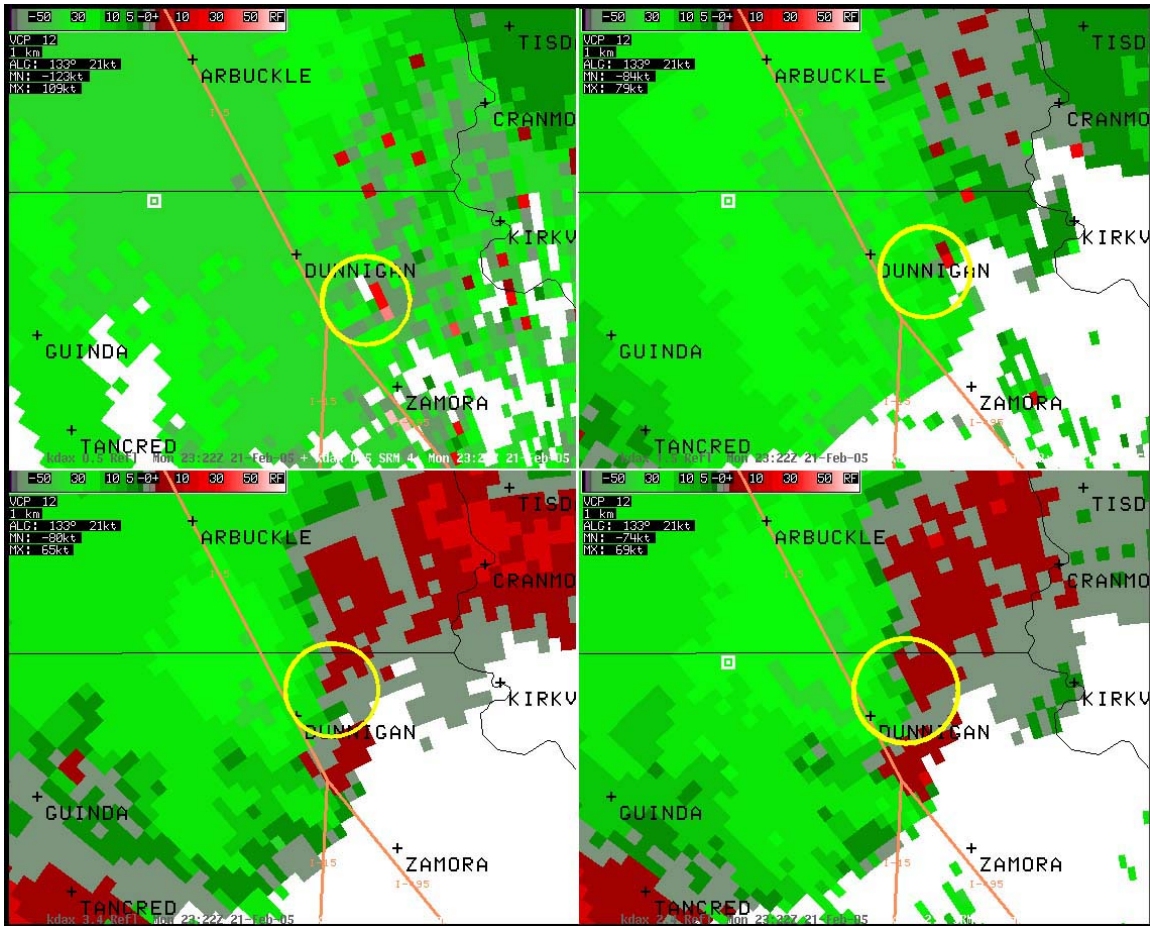


Figure 27b  
 WSR-88D Davis, CA (KDAY) 2322Z 21 February 2005 Storm Relative Motion  
 (SRM) Four Panel, 0.5 deg (UL), 1.3 deg (UR), 2.4 deg (LR), 3.1 deg (LL).  
 Yellow circle indicates mesocyclone.

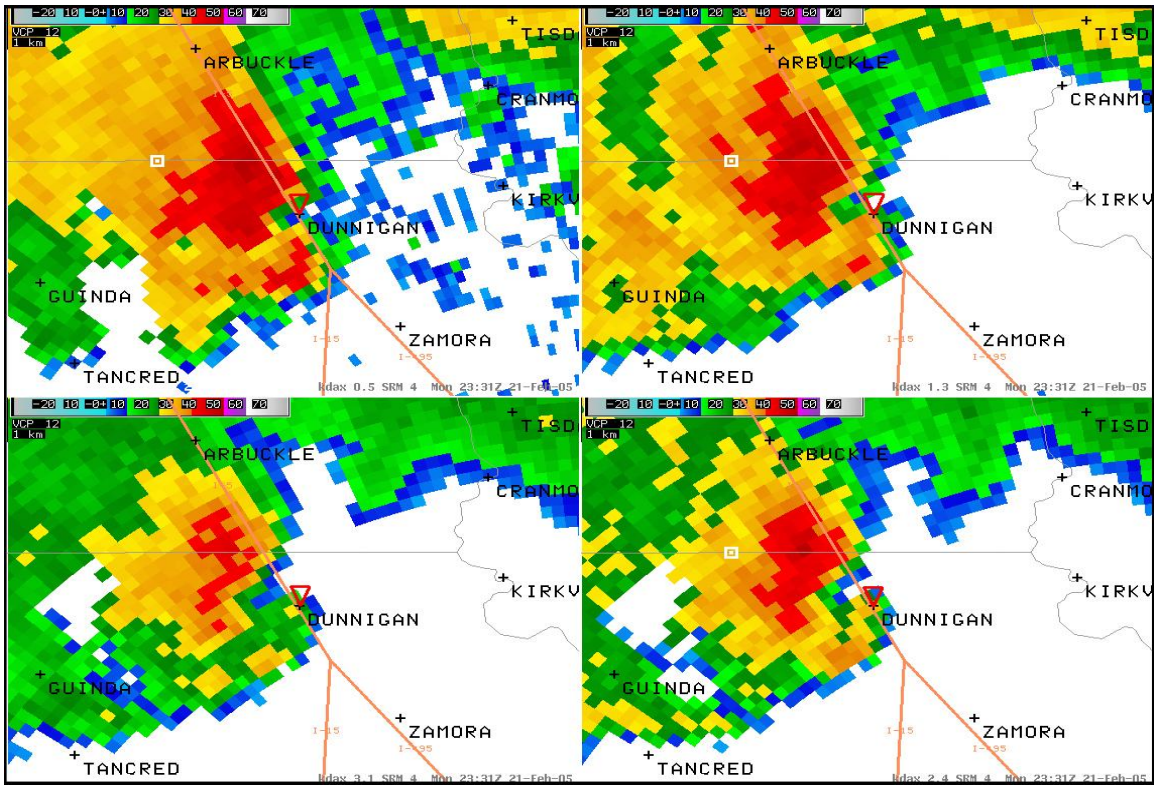


Figure 28a  
 WSR-88D Davis, CA (KDAX) 2331Z 21 February 2005 Storm Relative Motion  
 (SRM) Four Panel, 0.5 deg (UL), 1.3 deg (UR), 2.4 deg (LR), 3.1 deg (LL)  
 Inverted red triangle indicates tornado location.

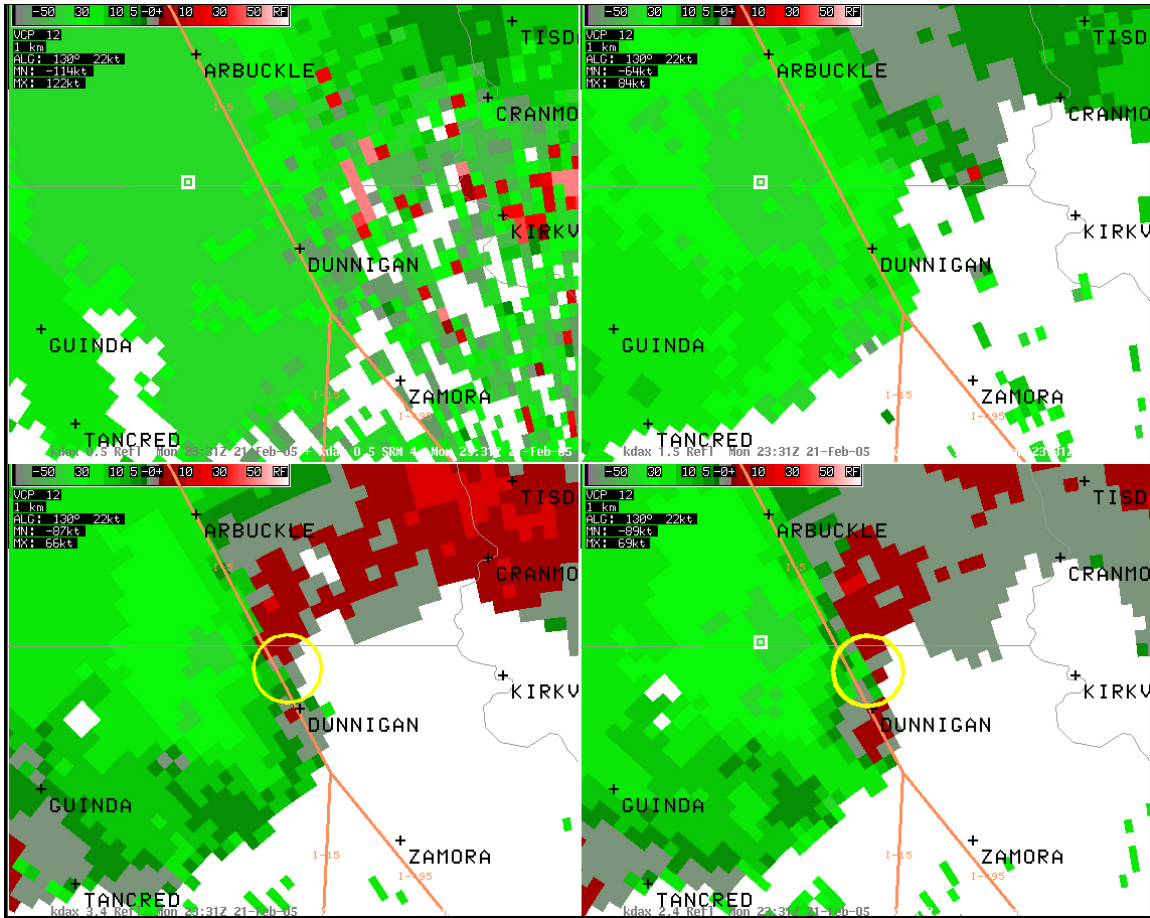


Figure 28b

*WSR-88D Davis, CA (KDAX) 2331Z 21 February 2005 Storm Relative Motion (SRM)  
 Four Panel, 0.5 deg (UL), 1.3 deg (UR), 2.4 deg (LR), 3.1 deg (LL).  
 Yellow circle indicates mesocyclone.*

Echo Tops (ET) products from the KDAX radar indicated a lowering of the storm's echo top. Research has documented how tornadoes from supercells occur during the lowering ("collapse") of the echo top and BWER (Lemon et al., 1979), and it is believed this happened in the Dunnigan, CA tornado. KDAX Echo Tops products (not shown) showed the echo tops lowering from 35,000 to 40,000 feet MSL at 2257Z and 2301Z, to 30,000 to 35,000 feet MSL from 2305Z to 2327Z, and to 25,000 to 30,000 feet MSL at 2331Z, well within the time frame when it is believed the Dunnigan, CA tornado occurred.

The 2.4 and 3.1 degree SRM elevation angles indicated the circulation maintained itself west of Interstate 5 through 2357Z (3:57 PM PST) as the thunderstorm continued to turn more westerly with time, and tracked westward along the Yolo/Colusa County line. The circulation did lower to the 1.5 degree elevation angle during the 2348Z (3:48 PM PST) volume scan (figure not shown), and remained evident in the radar imagery through the 2357Z (3:57 PM PST) volume scan (figure not shown). However, it is uncertain if another tornado occurred.

The continuity and depth of the mesocyclone, and the strength of the rotational velocities were greater with the Dunnigan, CA tornado than with the Natomas, CA or Southport, CA tornadoes. Considering the rotational continuity in the mid-levels and the formation and lowering of the mid-level mesocyclone and eventual tornado, the Dunnigan, CA tornado is believed to have followed the supercell cascade conceptual model outlined by Monteverdi et al. (2001). WSR-88D Reflectivity data show a Bounded Weak Echo Region (BWER) created by the advection of precipitation around the updraft area in Figures 24a, 26a, 27a and 28a. Also, the WSR-88D SRM data show a persistent mesocyclone, lasting over an hour in Figures 24b, 26b, 27b and 28b. The rear-flank downdraft (RFD) interacted with higher helicity values to the south (Figs. 21a-21c) and likely contributed to tornado formation. It is believed that the initial merging of thunderstorm cells (Fig. 24a) precluded tornado development, but was then followed by storm reorganization and re-intensification to produce the strongest tornado that day (Fig. 23).

#### 4. SUMMARY

The synoptic pattern on 21 February 2005 favored the development of thunderstorms in the Central Valley of California with the potential for low-topped or miniature supercells. Three of the thirteen tornadoes that occurred during the year in northern California occurred on this date. Fortunately, there were no fatalities or serious injuries from the tornadic thunderstorms.

The Southport, CA and Natomas, CA tornadoes occurred in heavily populated areas in the Sacramento area, and were highly witnessed and photographed by the public. These two tornadoes developed rapidly and early in the thunderstorm stage, and were classified as F0. The Southport, CA tornado was likely mesocyclonic, and the result of low level horizontal vorticity becoming tilted and stretched vertically along a boundary. The Natomas and Dunnigan, CA tornadoes were determined to have originated from the supercell cascade process conceptual model. The continuity and strength of the low-level mesocyclone was greater with the Dunnigan, CA tornado.

One unique characteristic was the location of a closed off mid- and upper-level vorticity maximum off the California coast that caused a deep southeast flow over northern California. This resulted in a typical anticyclonically-curving loop of the thunderstorm hodograph. However, the wind shear vectors were uniquely located in the upper left quadrant of the hodograph.

The Presidents' Day 2005 tornadoes in the central valley of northern California illustrated the importance of monitoring the storm environment and WSR-88D reflectivity and velocity products in anticipating and warning for tornadic storms. Forecasters can heighten their situational awareness by (i) monitoring the position and movement of low-level convergence boundaries, and (ii) by looking for small circulations along boundaries that show continuity and are developing and strengthening vertically near developing storms. Following this strategy can assist the forecaster in detecting potential circulations in low-topped supercell thunderstorms that may produce weak tornadoes.

Acknowledgements: The author is deeply appreciative of the tedious work by Mr. Jared Leighton (Meteorologist/Forecaster WFO Topeka, Ks) for masterfully creating the images, to Mr. John Juskie (former Science and Operations Officer NWS WFO Sacramento, CA), Mr. Daniel Kozlowski (HAS Forecaster, NWS CNRFC Sacramento, CA), and Mr. Paul Schlatter (Meteorologist/Instructor, NWS/OCWWS/ TD/ WDTB) for their expert review and comments which improved the meteorological quality of this study, and to Miss Katie Giannecchini for reviewing the paper, and to Ms. Elizabeth Morse (Retired MIC NWS WFO Sacramento, CA) for her encouragement to complete the study.

#### REFERENCES:

Blier, W., and K.A. Batten, 1994: On the incidence of tornadoes in California. *Wea.Forecasting*, **9**, 301-315.

Brady, R.H., and E. Szoke, 1988: The landspout - A common type of northeast Colorado tornado. *Preprints, 15th Conf. on Severe Local Storms*, Baltimore, MD, Amer. Meteor. Soc., 312-315.

Broyles, C., N. Dipasquale, and R. Wynne, 2002: JP1.4 Synoptic and mesoscale patterns associated with violent tornadoes across separate geographic regions of the United States: Part 1- low level characteristics. *21<sup>st</sup> AMS Conf. on Severe Local Storms*. San Antonio, TX, Amer. Meteor. Soc., **19**, J65-J68.

Bunkers, M.J., B.A. Klimowski, J.W. Zeitler, R.L. Thompson, and M.L. Weisman, 2000: Predicting supercell motion using a new hodograph technique. *Wea. Forecasting*, **15**, 61-79.

Burgess, D.W. and R.J. Donaldson, and P.R. Desrochers, 1993: Tornado detection and warning by radar. *The Tornado: Its Structure, Dynamics, Prediction, and Hazards, Geophys. Monogr. 79*, Amer. Geophys. Union, 203-221.

Carbone, R.E., 1982: A severe frontal rainband. Part I: Stormwide hydrodynamic structure. *J. Atmos. Sci.*, **39**, 258-279.

Choy, B.K., and S.M. Spratt, 1994: A WSR-88D approach to waterspout forecasting. NOAA Tech. Memo. NWS SR-156. 25 pp.

Craven, J.P., H.E. Brooks, and J.A. Hart, 2002: Baseline climatology of sounding derived parameters associated with deep, moist convection. *Preprints, 21<sup>st</sup> AMS Conf. on Severe Local Storms*. San Antonio, TX.

Crook, N.A., and M.W. Moncrieff, 1991: The Denver cyclone. Part II: Interaction with the convective boundary layer. *J. Atmos. Sci.*, **48**, 2109-2126.

Davies, J.M., 1993: Small tornadic supercells in the central plains. *Preprints, 17<sup>th</sup> Conf. on Severe Local Storms*, St. Louis, MO, Amer. Meteor. Soc., 305-309.

Fujita, T.T., 1981: Tornadoes and downbursts in the context of generalized planetary scales. *J. Atmos. Sci.*, **38**, 1511-1534.

Johns, R.H., J.C. Broyles, D. Eastlack, H. Guerrero, K. Harding, 2000: The role of synoptic patterns and temperature and moisture distribution in determining the locations of strong and violent tornado episodes in the north central United States: a preliminary examination. *Preprints, 20<sup>th</sup> Conf. on Severe Local Storms*. Orlando, FL, Amer. Meteor. Soc., 489-492.

Lemon, L.R., and C.A. Doswell III, 1979: Severe thunderstorm evolution and mesocyclone structure as related to tornadogenesis. *Mon. Wea. Rev.* **107**, 1184-1197.

Lindsey, D.T., and M.J. Bunkers, 2005: Observations of a severe, left-moving supercell on 4 May 2003. *Mon. Wea. Rev.* **20**, 15-22.

Lipari, G.S., and J.P. Monteverdi, 2000: Convective and shear parameters associated with northern and central California tornadoes during the period 1990-1994. *Preprints, 20<sup>th</sup> Conf. on Severe Local Storms*. Orlando, FL, Amer. Meteor. Soc., 518-521.

Markowski, P.M., E.N. Rasmussen, J.M. Straka, 1998: The occurrence of tornadoes in supercells interacting with boundaries during VORTEX-95. *Wea. Forecasting*, **13**, 852-859.

\_\_\_\_\_, J.M. Straka, E.N. Rasmussen, and D.O. Blanchard, 1998: Variability of storm-relative helicity during VORTEX. *Mon. Wea. Rev.* **126**, 2959-2971.

Marquis, J.N., Y.P. Richardson, and J.M. Wurman, 2004: Observations of mesocyclones along boundaries during IHOP. *Preprints, 22nd Conf. on Severe Local Storms*, Hyannis, MA.

Monteverdi, J.P., and S.A. Braun, 1988: An investigation of the 24 September 1986 "cold sector" tornado outbreak in northern California. National Weather Service Western Region Tech. Mem., NWS-203, 52 pp.

\_\_\_\_\_, J. Quadros, 1994: Convective and rotational parameters associated with three tornado episodes in northern and central California. *Wea. Forecasting*, **9**, 285-300.

\_\_\_\_\_, W. Blier, G. Stumpf, W. Pi, and K. Anderson, 2001: First WSR-88D documentation of an anticyclonic supercell with anticyclonic tornadoes: The Sunnyvale-LosAltos, California, tornadoes of 4 May 1998, *Mon. Wea. Rev.*, **129**, 2805-2814.

\_\_\_\_\_, C. Doswell III, and G.S. Lipari, 2003: Shear parameter thresholds for forecasting tornadic thunderstorms in northern and central California. *Wea. Forecasting*, **18**, 357-370.

Mueller, C.K., and R.E. Carbone, 1987: Dynamics of a thunderstorm outflow. *J. Atmos. Sci.*, **44**, 1879-1898.

Rasmussen, E.N., S. Richardson, J.M. Straka, P.M. Markowski, and D.O. Blanchard, 2000: The association of significant tornadoes with a baroclinic boundary on 2 June 1995, *Mon. Wea. Rev.* **128**, 174-191.

Smith, R. 1996: Non-supercell tornadoes: A review for forecasters. NOAA Tech. Memo. NWS SR-96-8, 6 pp.

Thompson, R.L., and R. Edwards, 2000: An overview of environmental conditions and forecast implications of the 3 May 1999 tornado outbreak. *Wea. Forecasting*, **15**, 682-699.

Wakimoto, R., and J.W. Wilson, 1989: Non-supercell tornadoes. *Mon. Wea. Rev.*, **117**, 1113-1140.

Wicker, L.J., and L. Cantrell, 1996: The role of vertical buoyancy distributions in miniature supercells. *Preprints, 18<sup>th</sup> Conf. on Severe Local Storms*. San Francisco, CA, Amer. Meteor. Soc., 225-229.

\_\_\_\_\_, and R.B. Wilhelmson, 1993: Numerical simulation of tornadogenesis within a supercell thunderstorm. *The Tornado: Its Structure, Dynamics, Prediction, and Hazards*, No. 79, *Geophys. Monogr.*, Amer. Geophys. Union, 75-88.

Wilson, J.W., 1986: Tornadogenesis by nonprecipitation induced by wind shear lines. *Mon. Wea. Rev.*, **114**, 270-284.

\_\_\_\_\_, G.B. Foote, N.A. Crook, J.C. Frankhauser, C.G. Wade, J.D. Tuttle, and D.K. Mueller, 1992: The role of boundary-layer convergence zones and horizontal rolls in the initiation of thunderstorms. A case study. *Mon. Wea. Rev.*, **120**, 1785-1815.

Wolf, R. 2002: Doppler radar observations of squall line tornadogenesis near the KDVN WSR-88D. *Preprints, 21<sup>st</sup> Conf. on Severe Local Storms*. San Antonio, TX.

Zeitler, J.W., and M.J. Bunkers, 2005: Operational forecasting of supercell motion: review and case studies using multiple datasets.



## NOAA TECHNICAL MEMORANDA National Weather Service, Western Region Subseries

The National Weather Service (NWS) Western Region (WR) Subseries provides an informal medium for the documentation and quick dissemination of results not appropriate, or not yet ready, for formal publication. The series is used to report on work in progress, to describe technical procedures and practices, or to relate

progress to a limited audience. These Technical Memoranda will report on investigations devoted primarily to regional and local problems of interest mainly to personnel, and hence will not be widely distributed.

Papers 1 to 25 are in the former series, ESSA Technical Memoranda, Western Region Technical Memoranda (WRTM); papers 24 to 59 are in the former series, ESSA Technical Memoranda, Weather Bureau Technical Memoranda (WBTM). Beginning with 60, the papers are part of the series, NOAA Technical Memoranda NWS. Out-of-print memoranda are not listed.

Papers 2 to 22, except for 5 (revised edition), are available from the National Weather Service Western Region, Scientific Services Division, 125 South State Street - Rm 1311, Salt Lake City, Utah 84138-1102. Paper 5 (revised edition), and all others beginning with 25 are available from the National Technical Information Service, U.S. Department of Commerce, Sills Building, 5285 Port Royal Road, Springfield, Virginia 22161. Prices vary for all paper copies; microfiche are \$3.50. Order by accession number shown in parentheses at end of each entry.

### ESSA Technical Memoranda (WRTM)

- 2 Climatological Precipitation Probabilities. Compiled by Lucianne Miller, December 1965.
- 3 Western Region Pre- and Post-FP-3 Program, December 1, 1965, to February 20, 1966. Edward D. Diemer, March 1966.
- 5 Station Descriptions of Local Effects on Synoptic Weather Patterns. Philip Williams, Jr., April 1966 (Revised November 1967, October 1969). (PB-17800)
- 8 Interpreting the RAREP. Herbert P. Benner, May 1966 (Revised January 1967).
- 11 Some Electrical Processes in the Atmosphere. J. Latham, June 1966.
- 17 A Digitalized Summary of Radar Echoes within 100 Miles of Sacramento, California. J. A. Youngberg and L. B. Overaas, December 1966.
- 21 An Objective Aid for Forecasting the End of East Winds in the Columbia Gorge, July through October. D. John Coparanis, April 1967.
- 22 Derivation of Radar Horizons in Mountainous Terrain. Roger G. Pappas, April 1967.

### ESSA Technical Memoranda, Weather Bureau Technical Memoranda (WBTM)

- 25 Verification of Operation Probability of Precipitation Forecasts, April 1966-March 1967. W. W. Dickey, October 1967. (PB-176240)
- 26 A Study of Winds in the Lake Mead Recreation Area. R. P. Augulis, January 1968. (PB-177830)
- 28 Weather Extremes. R. J. Schmidli, April 1968 (Revised March 1986). (PB86 177672/AS). (Revised October 1991 - PB92-115062/AS)
- 29 Small-Scale Analysis and Prediction. Philip Williams, Jr., May 1968. (PB178425)
- 30 Numerical Weather Prediction and Synoptic Meteorology. CPT Thomas D. Murphy, USAF, May 1968. (AD 673365)
- 31 Precipitation Detection Probabilities by Salt Lake ARTC Radars. Robert K. Belesky, July 1968. (PB 179084)
- 32 Probability Forecasting--A Problem Analysis with Reference to the Portland Fire Weather District. Harold S. Ayer, July 1968. (PB 179289)
- 36 Temperature Trends in Sacramento--Another Heat Island. Anthony D. Lentini, February 1969. (PB 183055)
- 37 Disposal of Logging Residues Without Damage to Air Quality. Owen P. Cramer, March 1969. (PB 183057)
- 39 Upper-Air Lows Over Northwestern United States. A.L. Jacobson, April 1969. PB 184296)
- 40 The Man-Machine Mix in Applied Weather Forecasting in the 1970s. L.W. Snellman, August 1969. (PB 185068)
- 43 Forecasting Maximum Temperatures at Helena, Montana. David E. Olsen, October 1969. (PB 185762)
- 44 Estimated Return Periods for Short-Duration Precipitation in Arizona. Paul C. Kangieser, October 1969. (PB 187763)
- 46 Applications of the Net Radiometer to Short-Range Fog and Stratus Forecasting at Eugene, Oregon. L. Yee and E. Bates, December 1969. (PB 190476)
- 47 Statistical Analysis as a Flood Routing Tool. Robert J.C. Burnash, December 1969. (PB 188744)
- 48 Tsunami. Richard P. Augulis, February 1970. (PB 190157)
- 49 Predicting Precipitation Type. Robert J.C. Burnash and Floyd E. Hug, March 1970. (PB 190962)

- 50 Statistical Report on Aeroallergens (Pollens and Molds) Fort Huachuca, Arizona, 1969. Wayne S. Johnson, April 1970. (PB 191743)
- 51 Western Region Sea State and Surf Forecaster's Manual. Gordon C. Shields and Gerald B. Burdwell, July 1970. (PB 193102)
- 52 Sacramento Weather Radar Climatology. R.G. Pappas and C. M. Veliquette, July 1970. (PB 193347)
- 54 A Refinement of the Vorticity Field to Delineate Areas of Significant Precipitation. Barry B. Aronovitch, August 1970.
- 55 Application of the SSARR Model to a Basin without Discharge Record. Vail Schermerhorn and Donal W. Kuehl, August 1970. (PB 194394)
- 56 Areal Coverage of Precipitation in Northwestern Utah. Philip Williams, Jr., and Werner J. Heck, September 1970. (PB 194389)
- 57 Preliminary Report on Agricultural Field Burning vs. Atmospheric Visibility in the Willamette Valley of Oregon. Earl M. Bates and David O. Chilcote, September 1970. (PB 194710)
- 58 Air Pollution by Jet Aircraft at Seattle-Tacoma Airport. Wallace R. Donaldson, October 1970. (COM 71 00017)
- 59 Application of PE Model Forecast Parameters to Local-Area Forecasting. Leonard W. Snellman, October 1970. (COM 71 00016)
- 60 An Aid for Forecasting the Minimum Temperature at Medford, Oregon, Arthur W. Fritz, October 1970. (COM 71 00120)
- 63 700-mb Warm Air Advection as a Forecasting Tool for Montana and Northern Idaho. Norris E. Woerner, February 1971. (COM 71 00349)
- 64 Wind and Weather Regimes at Great Falls, Montana. Warren B. Price, March 1971.
- 65 Climate of Sacramento, California. Laura Masters-Bevan. NWSO Sacramento, November 1998 (6<sup>th</sup> Revision). (PB99-118424)
- 66 A Preliminary Report on Correlation of ARTCC Radar Echoes and Precipitation. Wilbur K. Hall, June 1971. (COM 71 00829)
- 69 National Weather Service Support to Soaring Activities. Ellis Burton, August 1971. (COM 71 00956)
- 71 Western Region Synoptic Analysis-Problems and Methods. Philip Williams, Jr., February 1972. (COM 72 10433)
- 74 Thunderstorms and Hail Days Probabilities in Nevada. Clarence M. Sakamoto, April 1972. (COM 72 10554)
- 75 A Study of the Low Level Jet Stream of the San Joaquin Valley. Ronald A. Willis and Philip Williams, Jr., May 1972. (COM 72 10707)
- 76 Monthly Climatological Charts of the Behavior of Fog and Low Stratus at Los Angeles International Airport. Donald M. Gales, July 1972. (COM 72 11140)
- 77 A Study of Radar Echo Distribution in Arizona During July and August. John E. Hales, Jr., July 1972. (COM 72 11136)
- 78 Forecasting Precipitation at Bakersfield, California, Using Pressure Gradient Vectors. Earl T. Riddiough, July 1972. (COM 72 11146)
- 79 Climate of Stockton, California. Robert C. Nelson, July 1972. (COM 72 10920)
- 80 Estimation of Number of Days Above or Below Selected Temperatures. Clarence M. Sakamoto, October 1972. (COM 72 10021)
- 81 An Aid for Forecasting Summer Maximum Temperatures at Seattle, Washington. Edgar G. Johnson, November 1972. (COM 73 10150)
- 82 Flash Flood Forecasting and Warning Program in the Western Region. Philip Williams, Jr., Chester L. Glenn, and Roland L. Raetz, December 1972, (Revised March 1978). (COM 73 10251)
- 83 A comparison of Manual and Semiautomatic Methods of Digitizing Analog Wind Records. Glenn E. Rasch, March 1973. (COM 73 10669)
- 86 Conditional Probabilities for Sequences of Wet Days at Phoenix, Arizona. Paul C. Kangieser, June 1973. (COM 73 11264)
- 87 A Refinement of the Use of K-Values in Forecasting Thunderstorms in Washington and Oregon. Robert Y.G. Lee, June 1973. (COM 73 11276)
- 89 Objective Forecast Precipitation Over the Western Region of the United States. Julia N. Paegle and Larry P. Kierulff, September 1973. (COM 73 11946/3AS)
- 91 Arizona "Eddy" Tornadoes. Robert S. Ingram, October 1973. (COM 73 10465)
- 92 Smoke Management in the Willamette Valley. Earl M. Bates, May 1974. (COM 74 11277/AS)
- 93 An Operational Evaluation of 500-mb Type Regression Equations. Alexander E. MacDonald, June 1974. (COM 74 11407/AS)
- 94 Conditional Probability of Visibility Less than One-Half Mile in Radiation Fog at Fresno, California. John D. Thomas, August 1974. (COM 74 11555/AS)
- 95 Climate of Flagstaff, Arizona. Paul W. Sorenson, and updated by Reginald W. Preston, January 1987. (PB87 143160/AS) (Revised August 2002 3<sup>rd</sup> Revision)
- 96 Map type Precipitation Probabilities for the Western Region. Glenn E. Rasch and Alexander E. MacDonald, February 1975. (COM 75 10428/AS)
- 97 Eastern Pacific Cut-Off Low of April 21-28, 1974. William J. Alder and George R. Miller, January 1976. (PB 250 711/AS)
- 98 Study on a Significant Precipitation Episode in Western United States. Ira S. Brenner, April 1976. (COM 75 10719/AS)
- 99 A Study of Flash Flood Susceptibility-A Basin in Southern Arizona. Gerald Williams, August 1975. (COM 75 11360/AS)
- 102 A Set of Rules for Forecasting Temperatures in Napa and Sonoma Counties. Wesley L. Tuft, October 1975. (PB 246 902/AS)

- 103 Application of the National Weather Service Flash-Flood Program in the Western Region. Gerald Williams, January 1976. (PB 253 053/AS)
- 104 Objective Aids for Forecasting Minimum Temperatures at Reno, Nevada, During the Summer Months. Christopher D. Hill, January 1976. (PB 252 866/AS)
- 105 Forecasting the Mono Wind. Charles P. Ruscha, Jr., February 1976. (PB 254 650)
- 106 Use of MOS Forecast Parameters in Temperature Forecasting. John C. Plankinton, Jr., March 1976. (PB 254 649)
- 107 Map Types as Aids in Using MOS PoPs in Western United States. Ira S. Brenner, August 1976. (PB 259 594)
- 108 Other Kinds of Wind Shear. Christopher D. Hill, August 1976. (PB 260 437/AS)
- 109 Forecasting North Winds in the Upper Sacramento Valley and Adjoining Forests. Christopher E. Fontana, September 1976. (PB 273 677/AS)
- 110 Cool Inflow as a Weakening Influence on Eastern Pacific Tropical Cyclones. William J. Denney, November 1976. (PB 264 655/AS)
- 112 The MAN/MOS Program. Alexander E. MacDonald, February 1977. (PB 265 941/AS)
- 113 Winter Season Minimum Temperature Formula for Bakersfield, California, Using Multiple Regression. Michael J. Oard, February 1977. (PB 273 694/AS)
- 114 Tropical Cyclone Kathleen. James R. Fors, February 1977. (PB 273 676/AS)
- 116 A Study of Wind Gusts on Lake Mead. Bradley Colman, April 1977. (PB 268 847)
- 117 The Relative Frequency of Cumulonimbus Clouds at the Nevada Test Site as a Function of K-Value. R.F. Quiring, April 1977. (PB 272 831)
- 118 Moisture Distribution Modification by Upward Vertical Motion. Ira S. Brenner, April 1977. (PB 268 740)
- 119 Relative Frequency of Occurrence of Warm Season Echo Activity as a Function of Stability Indices Computed from the Yucca Flat, Nevada, Rawinsonde. Darryl Randerson, June 1977. (PB 271 290/AS)
- 121 Climatological Prediction of Cumulonimbus Clouds in the Vicinity of the Yucca Flat Weather Station. R.F. Quiring, June 1977. (PB 271 704/AS)
- 122 A Method for Transforming Temperature Distribution to Normality. Morris S. Webb, Jr., June 1977. (PB 271 742/AS)
- 124 Statistical Guidance for Prediction of Eastern North Pacific Tropical Cyclone Motion - Part I. Charles J. Neumann and Preston W. Leftwich, August 1977. (PB 272 661)
- 125 Statistical Guidance on the Prediction of Eastern North Pacific Tropical Cyclone Motion - Part II. Preston W. Leftwich and Charles J. Neumann, August 1977. (PB 273 155/AS)
- 126 Climate of San Francisco. E. Jan Null, February 1978. (Revised by George T. Pericht, April 1988 and January 1995). (PB88 208624/AS)
- 127 Development of a Probability Equation for Winter-Type Precipitation Patterns in Great Falls, Montana. Kenneth B. Mielke, February 1978. (PB 281 387/AS)
- 128 Hand Calculator Program to Compute Parcel Thermal Dynamics. Dan Gudel, April 1978. (PB 283 080/AS)
- 129 Fire whirls. David W. Goens, May 1978. (PB 283 866/AS)
- 130 Flash-Flood Procedure. Ralph C. Hatch and Gerald Williams, May 1978. (PB 286 014/AS)
- 131 Automated Fire-Weather Forecasts. Mark A. Mollner and David E. Olsen, September 1978. (PB 289 916/AS)
- 132 Estimates of the Effects of Terrain Blocking on the Los Angeles WSR-74C Weather Radar. R.G. Pappas, R.Y. Lee, B.W. Finke, October 1978. (PB 289767/AS)
- 133 Spectral Techniques in Ocean Wave Forecasting. John A. Jannuzzi, October 1978. (PB291317/AS)
- 134 Solar Radiation. John A. Jannuzzi, November 1978. (PB291195/AS)
- 135 Application of a Spectrum Analyzer in Forecasting Ocean Swell in Southern California Coastal Waters. Lawrence P. Kierulff, January 1979. (PB292716/AS)
- 136 Basic Hydrologic Principles. Thomas L. Dietrich, January 1979. (PB292247/AS)
- 137 LFM 24-Hour Prediction of Eastern Pacific Cyclones Refined by Satellite Images. John R. Zimmerman and Charles P. Ruscha, Jr., January 1979. (PB294324/AS)
- 138 A Simple Analysis/Diagnosis System for Real Time Evaluation of Vertical Motion. Scott Heflick and James R. Fors, February 1979. (PB294216/AS)
- 139 Aids for Forecasting Minimum Temperature in the Wenatchee Frost District. Robert S. Robinson, April 1979. (PB298339/AS)
- 140 Influence of Cloudiness on Summertime Temperatures in the Eastern Washington Fire Weather district. James Holcomb, April 1979. (PB298674/AS)
- 141 Comparison of LFM and MFM Precipitation Guidance for Nevada During Doreen. Christopher Hill, April 1979. (PB298613/AS)
- 142 The Usefulness of Data from Mountaintop Fire Lookout Stations in Determining Atmospheric Stability. Jonathan W. Corey, April 1979. (PB298899/AS)
- 143 The Depth of the Marine Layer at San Diego as Related to Subsequent Cool Season Precipitation Episodes in Arizona. Ira S. Brenner, May 1979. (PB298817/AS)
- 144 Arizona Cool Season Climatological Surface Wind and Pressure Gradient Study. Ira S. Brenner, May 1979. (PB298900/AS)
- 146 The BART Experiment. Morris S. Webb, October 1979. (PB80 155112)
- 147 Occurrence and Distribution of Flash Floods in the Western Region. Thomas L. Dietrich, December 1979. (PB80 160344)
- 149 Misinterpretations of Precipitation Probability Forecasts. Allan H. Murphy, Sarah Lichtenstein, Baruch Fischhoff, and Robert L. Winkler, February 1980. (PB80 174576)
- 150 Annual Data and Verification Tabulation - Eastern and Central North Pacific Tropical Storms and Hurricanes 1979. Emil B. Gunther and Staff, EPHC, April 1980. (PB80 220486)
- 151 NMC Model Performance in the Northeast Pacific. James E. Overland, PMEL-ERL, April 1980. (PB80 196033)
- 152 Climate of Salt Lake City, Utah. William J. Alder, Sean T. Buchanan, William Cope (Retired), James A. Cisco, Craig C. Schmidt, Alexander R. Smith (Retired), Wilbur E. Figgins (Retired), February 1998 - Seventh Revision (PB98-130727)
- 153 An Automatic Lightning Detection System in Northern California. James E. Rea and Chris E. Fontana, June 1980. (PB80 225592)
- 154 Regression Equation for the Peak Wind Gust 6 to 12 Hours in Advance at Great Falls During Strong Downslope Wind Storms. Michael J. Oard, July 1980. (PB91 108367)
- 155 A Raininess Index for the Arizona Monsoon. John H. Ten Harkel, July 1980. (PB81 106494)
- 156 The Effects of Terrain Distribution on Summer Thunderstorm Activity at Reno, Nevada. Christopher Dean Hill, July 1980. (PB81 102501)
- 157 An Operational Evaluation of the Scofield/Oliver Technique for Estimating Precipitation Rates from Satellite Imagery. Richard Ochoa, August 1980. (PB81 108227)
- 158 Hydrology Practicum. Thomas Dietrich, September 1980. (PB81 134033)
- 159 Tropical Cyclone Effects on California. Arnold Court, October 1980. (PB81 133779)
- 160 Eastern North Pacific Tropical Cyclone Occurrences During Intraseasonal Periods. Preston W. Leftwich and Gail M. Brown, February 1981. (PB81 205494)
- 161 Solar Radiation as a Sole Source of Energy for Photovoltaics in Las Vegas, Nevada, for July and December. Darryl Randerson, April 1981. (PB81 224503)
- 162 A Systems Approach to Real-Time Runoff Analysis with a Deterministic Rainfall-Runoff Model. Robert J.C. Burnash and R. Larry Ferral, April 1981. (PB81 224495)
- 163 A Comparison of Two Methods for Forecasting Thunderstorms at Luke Air Force Base, Arizona. LTC Keith R. Cooley, April 1981. (PB81 225393)
- 164 An Objective Aid for Forecasting Afternoon Relative Humidity Along the Washington Cascade East Slopes. Robert S. Robinson, April 1981. (PB81 23078)
- 165 Annual Data and Verification Tabulation, Eastern North Pacific Tropical Storms and Hurricanes 1980. Emil B. Gunther and Staff, May 1981. (PB82 230336)
- 166 Preliminary Estimates of Wind Power Potential at the Nevada Test Site. Howard G. Booth, June 1981. (PB82 127036)
- 167 ARAP User's Guide. Mark Mathewson, July 1981, Revised September 1981. (PB82 196783)
- 168 Forecasting the Onset of Coastal Gales Off Washington-Oregon. John R. Zimmerman and William D. Burton, August 1981. (PB82 127051)
- 169 A Statistical-Dynamical Model for Prediction of Tropical Cyclone Motion in the Eastern North Pacific Ocean. Preston W. Leftwich, Jr., October 1981. (PB82195298)
- 170 An Enhanced Plotter for Surface Airways Observations. Andrew J. Spry and Jeffrey L. Anderson, October 1981. (PB82 153883)
- 171 Verification of 72-Hour 500-MB Map-Type Predictions. R.F. Quiring, November 1981. (PB82-158098)
- 172 Forecasting Heavy Snow at Wenatchee, Washington. James W. Holcomb, December 1981. (PB82-177783)
- 173 Central San Joaquin Valley Type Maps. Thomas R. Crossan, December 1981. (PB82 196064)
- 174 ARAP Test Results. Mark A. Mathewson, December 1981. (PB82 198103)
- 176 Approximations to the Peak Surface Wind Gusts from Desert Thunderstorms. Darryl Randerson, June 1982. (PB82 253089)
- 177 Climate of Phoenix, Arizona. Robert J. Schmidli and Austin Jamison, April 1969 (Revised July 1996). (PB96-191614)
- 178 Annual Data and Verification Tabulation, Eastern North Pacific Tropical Storms and Hurricanes 1982. E.B. Gunther, June 1983. (PB85 106078)
- 179 Stratified Maximum Temperature Relationships Between Sixteen Zone Stations in Arizona and Respective Key Stations. Ira S. Brenner, June 1983. (PB83 249904)
- 180 Standard Hydrologic Exchange Format (SHEF) Version I. Phillip A. Pasteris, Vernon C. Bissel, David G. Bennett, August 1983. (PB85 106052)
- 181 Quantitative and Spacial Distribution of Winter Precipitation along Utah's Wasatch Front. Lawrence B. Dunn, August 1983. (PB85 106912)
- 182 500 Millibar Sign Frequency Teleconnection Charts - Winter. Lawrence B. Dunn, December 1983. (PB85 106276)
- 183 500 Millibar Sign Frequency Teleconnection Charts - Spring. Lawrence B. Dunn, January 1984. (PB85 111367)

- 184 Collection and Use of Lightning Strike Data in the Western U.S. During Summer 1983. Glenn Rasch and Mark Mathewson, February 1984. (PB85 110534)
- 185 500 Millibar Sign Frequency Teleconnection Charts - Summer. Lawrence B. Dunn, March 1984. (PB85 111359)
- 186 Annual Data and Verification Tabulation eastern North Pacific Tropical Storms and Hurricanes 1983. E.B. Gunther, March 1984. (PB85 109635)
- 187 500 Millibar Sign Frequency Teleconnection Charts - Fall. Lawrence B. Dunn, May 1984. (PB85-110930)
- 188 The Use and Interpretation of Isentropic Analyses. Jeffrey L. Anderson, October 1984. (PB85-132694)
- 189 Annual Data & Verification Tabulation Eastern North Pacific Tropical Storms and Hurricanes 1984. E.B. Gunther and R.L. Cross, April 1985. (PB85 1878887AS)
- 190 Great Salt Lake Effect Snowfall: Some Notes and An Example. David M. Carpenter, October 1985. (PB86 119153/AS)
- 191 Large Scale Patterns Associated with Major Freeze Episodes in the Agricultural Southwest. Ronald S. Hamilton and Glenn R. Lussky, December 1985. (PB86 144474AS)
- 192 NWR Voice Synthesis Project: Phase I. Glen W. Sampson, January 1986. (PB86 145604/AS)
- 193 The MCC - An Overview and Case Study on Its Impact in the Western United States. Glenn R. Lussky, March 1986. (PB86 170651/AS)
- 194 Annual Data and Verification Tabulation Eastern North Pacific Tropical Storms and Hurricanes 1985. E.B. Gunther and R.L. Cross, March 1986. (PB86 170941/AS)
- 195 Radid Interpretation Guidelines. Roger G. Pappas, March 1986. (PB86 177680/AS)
- 196 A Mesoscale Convective Complex Type Storm over the Desert Southwest. Darryl Randerson, April 1986. (PB86 190998/AS)
- 197 The Effects of Eastern North Pacific Tropical Cyclones on the Southwestern United States. Walter Smith, August 1986. (PB87 106258AS)
- 198 Preliminary Lightning Climatology Studies for Idaho. Christopher D. Hill, Carl J. Gorski, and Michael C. Conger, April 1987. (PB87 180196/AS)
- 199 Heavy Rains and Flooding in Montana: A Case for Slantwise Convection. Glenn R. Lussky, April 1987. (PB87 185229/AS)
- 200 Annual Data and Verification Tabulation Eastern North Pacific Tropical Storms and Hurricanes 1986. Roger L. Cross and Kenneth B. Mielke, September 1987. (PB88 110895/AS)
- 201 An Inexpensive Solution for the Mass Distribution of Satellite Images. Glen W. Sampson and George Clark, September 1987. (PB88 114038/AS)
- 202 Annual Data and Verification Tabulation Eastern North Pacific Tropical Storms and Hurricanes 1987. Roger L. Cross and Kenneth B. Mielke, September 1988. (PB88-101935/AS)
- 203 An Investigation of the 24 September 1986 "Cold Sector" Tomado Outbreak in Northern California. John P. Monteverti and Scott A. Braun, October 1988. (PB89 121297/AS)
- 204 Preliminary Analysis of Cloud-To-Ground Lightning in the Vicinity of the Nevada Test Site. Carven Scott, November 1988. (PB89 128649/AS)
- 205 Forecast Guidelines For Fire Weather and Forecasters -- How Nighttime Humidity Affects Wildland Fuels. David W. Goens, February 1989. (PB89 162549/AS)
- 206 A Collection of Papers Related to Heavy Precipitation Forecasting. Western Region Headquarters, Scientific Services Division, August 1989. (PB89 230833/AS)
- 207 The Las Vegas McCarran International Airport Microburst of August 8, 1989. Carven A. Scott, June 1990. (PB90-240268)
- 208 Meteorological Factors Contributing to the Canyon Creek Fire Blowup, September 6 and 7, 1988. David W. Goens, June 1990. (PB90-245085)
- 209 Stratus Surge Prediction Along the Central California Coast. Peter Felsch and Woodrow Whitlatch, December 1990. (PB91-129239)
- 210 Hydrotools. Tom Egger, January 1991. (PB91-151787/AS)
- 211 A Northern Utah Soaker. Mark E. Struthwolf, February 1991. (PB91-168716)
- 212 Preliminary Analysis of the San Francisco Rainfall Record: 1849-1990. Jan Null, May 1991. (PB91-208439)
- 213 Idaho Zone Preformat, Temperature Guidance, and Verification. Mark A. Mollner, July 1991. (PB91-227405/AS)
- 214 Emergency Operational Meteorological Considerations During an Accidental Release of Hazardous Chemicals. Peter Mueller and Jerry Galt, August 1991. (PB91-235424)
- 215 WeatherTools. Tom Egger, October 1991. (PB93-184950)
- 216 Creating MOS Equations for RAWs Stations Using Digital Model Data. Dennis D. Gettman, December 1991. (PB92-131473/AS)
- 217 Forecasting Heavy Snow Events in Missoula, Montana. Mike Richmond, May 1992. (PB92-196104)
- 218 NWS Winter Weather Workshop in Portland, Oregon. Various Authors, December 1992. (PB93-146785)
- 219 A Case Study of the Operational Usefulness of the Sharp Workstation in Forecasting a Mesocyclone-Induced Cold Sector Tornado Event in California. John P. Monteverti, March 1993. (PB93-178697)
- 220 Climate of Pendleton, Oregon. Claudia Bell, August 1993. (PB93-227536)
- 221 Utilization of the Bulk Richardson Number, Helicity and Sounding Modification in the Assessment of the Severe Convective Storms of 3 August 1992. Eric C. Evenson, September 1993. (PB94-131943)
- 222 Convective and Rotational Parameters Associated with Three Tornado Episodes in Northern and Central California. John P. Monteverti and John Quadros, September 1993. (PB94-131943)
- 223 Climate of San Luis Obispo, California. Gary Ryan, February 1994. (PB94-162062)
- 224 Climate of Wenatchee, Washington. Michael W. McFarland, Roger G. Buckman, and Gregory E. Matzen, March 1994. (PB94-164308)
- 225 Climate of Santa Barbara, California. Gary Ryan, December 1994. (PB95-173720)
- 226 Climate of Yakima, Washington. Greg DeVoir, David Hogan, and Jay Neher, December 1994. (PB95-173688)
- 227 Climate of Kalispell, Montana. Chris Maier, December 1994. (PB95-169488)
- 228 Forecasting Minimum Temperatures in the Santa Maria Agricultural District. Wilfred Pi and Peter Felsch, December 1994. (PB95-171088)
- 229 The 10 February 1994 Oroville Tornado--A Case Study. Mike Staudenmaier, Jr., April 1995. (PB95-241873)
- 230 Santa Ana Winds and the Fire Outbreak of Fall 1993. Ivory Small, June 1995. (PB95-241865)
- 231 Washington State Tornadoes. Tresté Huse, July 1995. (PB96-107024)
- 232 Fog Climatology at Spokane, Washington. Paul Frisbie, July 1995. (PB96-106604)
- 233 Storm Relative Isentropic Motion Associated with Cold Fronts in Northern Utah. Kevin B. Baker, Kathleen A. Hadley, and Lawrence B. Dunn, July 1995. (PB96-106596)
- 234 Some Climatological and Synoptic Aspects of Severe Weather Development in the Northwestern United States. Eric C. Evenson and Robert H. Johns, October 1995. (PB96-112958)
- 235 Climate of Las Vegas, Nevada. Paul H. Skrbac and Scott Cordero, December 1995. (PB96-135553)
- 236 Climate of Astoria, Oregon. Mark A. McInerney, January 1996.
- 237 The 6 July 1995 Severe Weather Events in the Northwestern United States: Recent Examples of SSWEs. Eric C. Evenson, April 1996.
- 238 Significant Weather Patterns Affecting West Central Montana. Joe Lester, May 1996. (PB96-178751)
- 239 Climate of Portland, Oregon. Clinton C. D. Rockey, May 1996. (PB96-17603) - First Revision, October 1999
- 240 Downslow Winds of Santa Barbara, CA. Gary Ryan, July 1996. (PB96-191697)
- 241 Operational Applications of the Real-time National Lightning Detection Network Data at the NWSO Tucson, AZ. Darren McCollum, David Bright, Jim Meyer, and John Glueck, September 1996. (PB97-108450)
- 242 Climate of Pocatello, Idaho. Joe Heim, October 1996. (PB97-114540)
- 243 Climate of Great Falls, Montana. Matt Jackson and D. C. Williamson, December 1996. (PB97-126684)
- 244 WSR-88D VAD Wind Profile Data Influenced by Bird Migration over the Southwest United States. Jesus A. Haro, January 1997. (PB97-135263)
- 245 Climatology of Cape for Eastern Montana and Northern Wyoming. Heath Hockenberry and Keith Meier, January 1997. (PB97-133425)
- 246 A Western Region Guide to the Eta-29 Model. Mike Staudenmaier, Jr., March 1997. (PB97-144075)
- 247 The Northeast Nevada Climate Book. Edwin C. Clark, March 1997. (First Revision - January 1998 - Andrew S. Gorelow and Edwin C. Clark - PB98-123250)
- 248 Climate of Eugene, Oregon. Clinton C. D. Rockey, April 1997. (PB97-155303)
- 249 Climate of Tucson, Arizona. John R. Glueck, October 1997
- 250 Northwest Oregon Daily Extremes and Normans. Clinton C. D. Rockey, October 1997
- 251 A Composite Study Examining Five Heavy Snowfall Patterns for South-Central Montana. Jonathan D. Van Aussdal and Thomas W. Humphrey, February 1998. (PB98-125255)
- 252 Climate of Eureka, California. Alan H. Puffer. February 1998. (PB98-130735)
- 253 Inferred Oceanic Kelvin/Rosby Wave Influence on North American West Coast Precipitation. Martin E. Lee and Dudley Chelton. April 1998. (PB98-139744)
- 254 Conditional Symmetric Instability: Methods of Operational Diagnosis and Case Study of 23-24 February 1994 Eastern Washington/Oregon Snowstorm. Gregory A. DeVoir. May 1998. (PB98-144660)
- 255 Creation and Maintenance of a Comprehensive Climate Data Base. Eugene Petrescu. August 1998. (PB98-173529)
- 256 Climate of San Diego, California. Thomas E. Evans, III and Donald A. Halvorsen. October 1998. (PB99-109381)
- 257 Climate of Seattle, Washington. Dana Felton. November 1998. (PB99-113482)
- 258 1985-1998 North Pacific Tropical Cyclones Impacting the Southwestern United States and Northern Mexico: An Updated Climatology. Armando L. Garza. January 1999. (PB99-130502)
- 259 Climate of San Jose, California. Miguel Miller. April 1999. (PB99-145633)
- 260 Climate of Las Vegas, Nevada. Paul H. Skrbac. December 1999
- 261 Climate of Los Angeles, California. David Bruno, Gary Ryan, with assistance from Curt Kaplan and Jonathan Slemmer. January 2000

- 262 Climate of Miles City, Montana. David A. Spector and Mark H. Strobin. April 2000
- 263 Analysis of Radiosonde Data for Spokane, Washington. Rocco D. Pelatti. November 2000
- 264 Climate of Billings, Montana. Jeffrey J. Zeltwanger and Mark H. Strobin. November 2000
- 265 Climate of Sheridan, Wyoming. Jeffrey J. Zeltwanger, Sally Springer, Mark H. Strobin. March 2001
- 266 Climate of Sacramento, California. Laura Masters-Bevan. December 2000 (7th Revision)
- 267 Sulphur Mountain Doppler Radar: A Performance Study. Los Angeles/Oxnard WFO. August 2001
- 268 Prediction of Heavy Snow Events in the Snake River Plain Using Pattern Recognition and Regression Techniques. Thomas Andretta and William Wojcik. October 2003
- 269 The Lewis and Clark Expedition 18-03-1806. Weather, Water and Climate, Vernon Preston, Pocatello Idaho, December 2004.
- 270 Climate of San Diego, California, Emmanuel M. Isla, September 2004 (2<sup>nd</sup> Edition)
- 271 Climate of Las Vegas, Nevada, Andrew S. Gorelow, January 2005, (2nd Edition)
- 272 Climate of Sacramento, California, Revised by: Laura A. Bevan and George Cline, June 2005
- 273 Climate of Flagstaff, AZ 4<sup>th</sup> Revision. Mike Staudenmaier, Jr, Reginald Preston(R), Paul Sorenson (R) , August 2005
- 274 Climate of Prescott, AZ, Bob Fogarty, Mike Staudenmaier Jr., Flagstaff WFO, AZ, August 2005.
- 275 Climate of San Diego, CA, 3<sup>rd</sup> Revision. Noel M. Isla, Jennifer Lee, March 2006
- 276 Climate of Reno, NV, Brian Ohara, Reno, NV October 2006
- 277 Forecaster's Handbook for Extreme Southwestern California Based On Short Term Climatological Approximations: Part I - The Marine Layer and Its Effect On Precipitation and Heating Ivory J. Small, October 2006
- 278 Forecaster's Handbook for Extreme Southwestern California Based On Short Term Climatological Approximations: Part II – Wind Effects on Terrestrial and Marine Environments Ivory J. Small, December 2006
- 279 Effects of Wildfire in the Mountainous Terrain of Southeast Arizona: An Empirical Formula to Estimate 5-Year Peak Discharge from Small Post-Burn Watersheds, William B. Reed and Mike Schaffner , June 2007
- 280 The Climate of Fresno, California, Chris Stachelski and Gary Sanger, March 2008
- 281 The Climate of Bakersfield, California, Chris Stachelski and Gary Sanger, February 2008
- 282 Hazardous Weather Climatology for Arizona, Craig Shoemaker and Jeffrey T. Davis, February 2008
- 283 Effects of Wildfire in the Mountainous Terrain of Southeast Arizona: Empirical Formulas to Estimate from 1-Year through 10-Year Peak Discharge from Post-Burn Watersheds, William B. Reed and Mike Schaffner, July 2008
- 284 The Presidents' Day 2005 Tornadoes in the Southern Sacramento Valley of Northern California, James H. Mathews, Sacramento, CA, September 2009

